A review talk to be presented at the WEIN-98 Conference, June 15-19, 1998, Santa Fe, NM
Draft: 6/8/98

Parity Nonconservation in Atoms

Dmitry Budker[§]
Department of Physics, University of California, Berkeley, and Nuclear Science Division,
Lawrence Berkeley National Laboratory, Berkeley, CA 94720-7300

Introduction

In 1959, many years before the discovery of the weak neutral currents, Yakov Borisovich Zel'dovich considered effects on an atom of a hypothetical electron-nucleon neutral current interaction with strength comparable to that of the charged-current parity-violating interaction [1]. He pointed out that the interference of a parity-nonconserving (PNC) neutral current interaction with the regular electromagnetic interaction in an atom should lead to polarization plane rotation of light passing through media not normally considered optically active. Estimating this effect for a 'generic' atomic sample, he came to a conclusion that the effect is so small that it "obviously cannot be observed". This was one of several occasions where Zel'dovich made a daring proposition, convinced himself of impossibility of its realization, and nevertheless, triggered development of a whole new direction in physics (one other example is the idea of colliding beams) [2]. In the case of atomic PNC, the trigger turned out to be delayed. It was not until 1974 when M.-A. Bouchiat and C. Bouchiat, motivated by new developments in weak interaction field theory and laser technology, reanalyzed atomic PNC and noted a large enhancement with atomic number Z, approximately proportional to Z^3, making the PNC effects actually large enough to be measurable in some heavy atoms [3]. The first observations were made using optical rotation in bismuth at Novosibirsk [4] and the Stark-interference technique (see below) in thallium at Berkeley [5]. These experiments played an important role in establishing the existence of electron-quark neutral current [6] which, in turn, helped establish the Standard Model of the electroweak interactions. Other PNC experiments with heavy atoms by groups in Paris, Oxford, Seattle, Moscow and Boulder have yielded final results agreeing with the predictions of the Standard Model of the electroweak interactions. Experimental uncertainty is now in the range .35-3% of the PNC effects, a remarkable progress from the results of the first experiments. The goals and motivation for atomic PNC experiments have changed as well. Modern experiments

provide quantitative tests of the Standard Model at small momentum transfer [7]. In addition, atomic PNC effects also allow observation of the nuclear-spin dependent PNC interactions dominated by the nuclear anapole moment [8,9]. Nuclear spin-dependent effects (which were recently unambiguously detected in an experiment with Cs [10]) provide new information about the neutral current weak interactions in the hadron sector which is difficult to obtain with other methods [11]. It has also been suggested that atomic PNC experiments could eventually be of use for a perhaps much more prosaic task of determination of neutron radii [12].

Several reviews of atomic PNC have been given in recent years, including a book [13], papers [14], and the most recent exhaustive article [15]. Here, the two most precise experiments so far will be briefly described, and then a review will be given of some new approaches to atomic PNC being developed by various groups. Finally, some proposals which are still at the level of ideas will be mentioned, followed by a conclusion on the status and the future of the field. Largely the interests of the author dictate the choice of the material in this paper. Many interesting topics are omitted by necessity due to limitations in space. This includes, e.g., parity violation in diatomic [16] and chiral [13,15] molecules.

Optical Rotation Experiments

Currently the most sensitive optical rotation experiments are the ones carried out by the groups at Oxford [17] (Bi, 876 nm transition, 2 % accuracy) and Seattle [18,19] (Tl, 1283 nm transition and Pb, 1279 nm transition, 1 % accuracy on both). In these experiments, the frequency of a laser is tuned to the vicinity of a magnetic dipole resonance. The PNC-mixing of states of opposite nominal parity induces an E1 transition amplitude. The interference between this PNC-induced E1 amplitude and the dominant M1 amplitude leads to natural optical activity on the order of 10^{-7} rad per resonant absorption length. The obvious difficulty of measuring such small rotation angles is augmented by the absence of any experimental reversals that would change the PNC effect without affecting the dominant transition amplitude and spurious rotations. Thus, in a precise PNC experiment (Fig. 1) one relies on detailed understanding of the complicated optical rotation lineshape (Fig. 2) and a number of additional tricks, like periodically substituting the real atomic vapor tube with an empty dummy tube to

suppress the influence of spurious rotations due to imperfections of the polarimeter. One may note that this traditional optical rotation technique is probably at the limit of its sensitivity. In fact, the actual sensitivity of measurements of optical rotation remains at the level ~10^{-8} radians, similar to that of the first experiments 20 years ago. The accuracy level achieved by the Oxford and Seattle groups is mainly due to an ingenious scheme in which the optical density of the atomic sample was greatly increased and measurements were carried out on the wing of an absorption line [20]. Therefore, it appears that in order to make further experimental progress in optical rotation measurements, radically new approaches are necessary. One such approach using Electromagnetically-Induced Transparency (EIT) is being pursued by the Seattle group. This is discussed in a subsequent section. Another approach involves a search for other, more exotic systems where optical rotation may be enhanced. Below we describe the efforts of various groups to find favorable transitions in the rare earth atoms. The use of the rare earth atoms with an abundance of stable isotopes with a broad variation of neutron numbers may also solve another problem. The interpretation of all precise PNC experiments is currently limited by atomic theory. Fort the optical rotation experiments, the theoretical uncertainty remains at a 3 % level for the best case of Tl [21], and is even worse for Pb and Bi, despite the continuing efforts to improve the theoretical accuracy for these atoms [22]. It has been suggested to avoid uncertainties in atomic theory by comparing PNC effects on different isotopes [23]. Several possible schemes for using isotope comparisons are discussed below. In [12], it was pointed out that current uncertainties in neutron distributions within the nucleus may ultimately limit the sensitivity of isotopic comparisons to fundamental weak interaction physics when these experiments reach the sub-1% level of sensitivity. This limitation may be overcome in the future by a combination of theoretical work and scattering experiments [24].

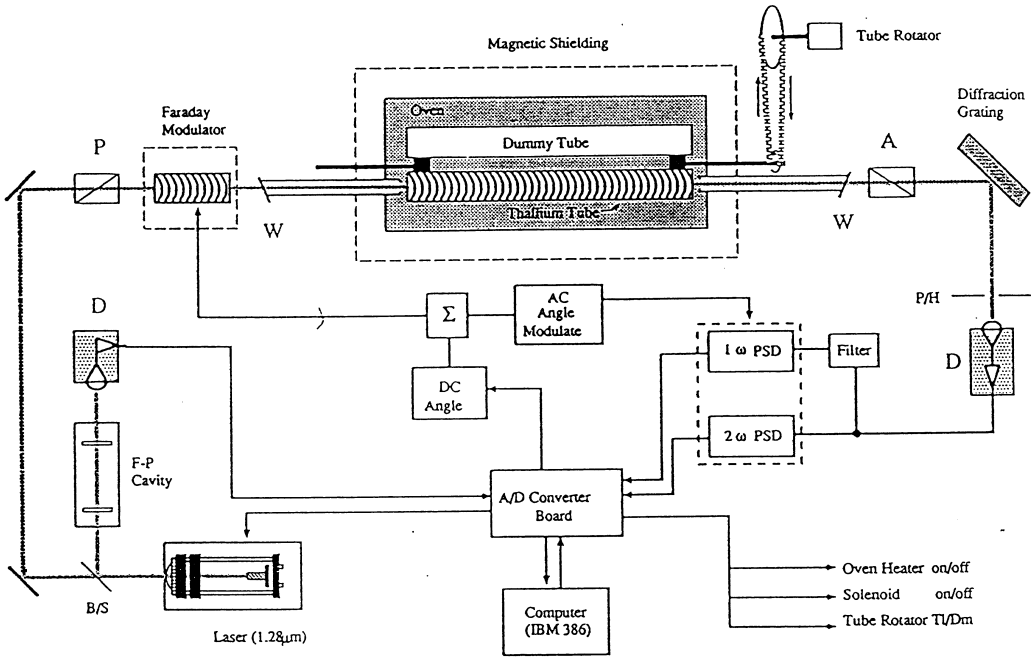

Fig. 1. Seattle polarimeter apparatus for measurements of PNC in Tl and Pb [19].

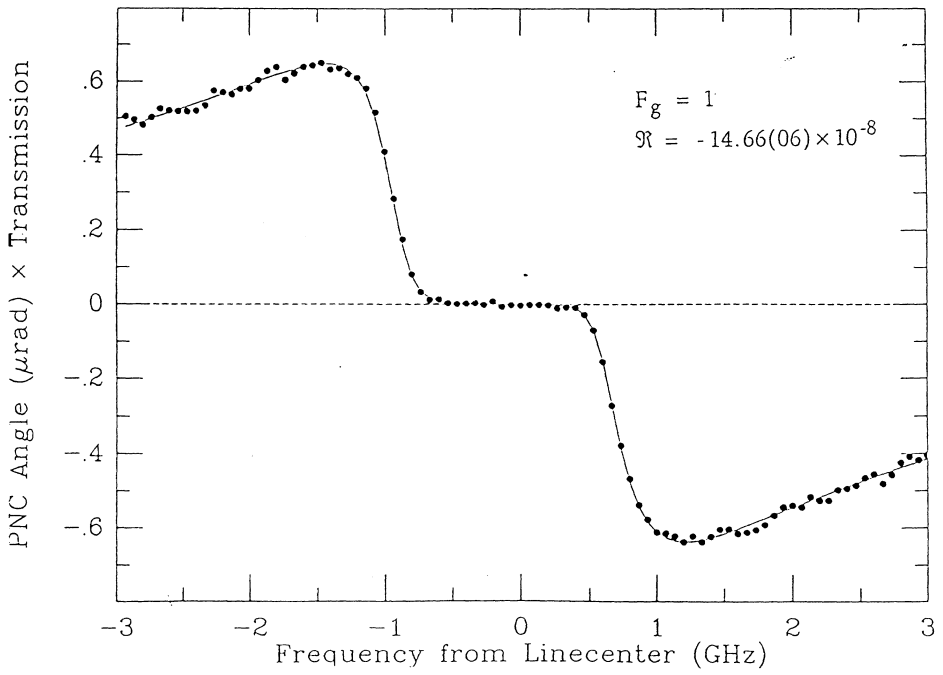

Fig. 2. Experimental lineshape of the PNC optical rotation in the Tl experiment [18]. The shown lineshape segment corresponds to the hyperfine transition components with the total angular momentum in the ground state F_g=1. The data represents 500 hrs of averaging.

Stark-PNC interference experiments in Cs; discovery of the nuclear anapole moment

Of recent atomic PNC experiments, the one that has the largest impact on particle and nuclear physics is the Boulder experiment with Cs [10]. The two main reasons for this are an unprecedented experimental precision of 0.35 % and the relatively simple atomic structure of Cs, for which high precision atomic calculations (1 %) have been carried out [25]. In this experiment, it was also possible to detect and measure, with a 14 % relative uncertainty, the minute difference in PNC amplitudes for different hyperfine components of the transition. This difference constitutes about 5 % of the leading PNC amplitude, and is, to a large extent, due to the nuclear anapole moment.

The anapole moment, first introduced by Zel'dovich and V. G. Vaks [8], is a parity-violating form factor that appears in the multipole moment expansion of the vector potential and leads to a contact interaction (see e.g. [26,13]):

$$\mathbf{A}^{\mathrm{a}}(\mathbf{r}) = \mathbf{a}\delta(\mathbf{r}); \quad \mathbf{a} = -\pi\int r^2 \mathbf{j}(\mathbf{r}) d^3 r\,, \tag{1}$$

where $\mathbf{A}^{\mathrm{a}}(\mathbf{r})$ is the vector potential due to the anapole, $\mathbf{j}(\mathbf{r})$ is the electromagnetic current, and $\mathbf{a}$ is the anapole moment. As is true for any rank-one tensor (vector) characteristic of a system (in this case an atomic nucleus) the anapole moment must be proportional to the total angular momentum of the system, **I**. The parity-violating nature of the anapole moment becomes apparent when one considers the behavior of $\mathbf{a}$ and **I** under spatial inversion: while the latter is a pseudo-vector, the former is a normal vector just like $\mathbf{j}(\mathbf{r})$. In order to visualize the simplest system possessing an anapole moment, first consider a current loop offset from the origin [26] (Fig. 3 a). Straight from the definition (1), there is a non-zero anapole moment pointing in the direction opposite to that of the current at a point furthest from the origin. A direct generalization of this is a toroidal winding (Fig. 3 b) where the current consecutively flows through a series of such loops [27].

In the early 1980's it was realized [9] that the nuclear anapole moment arising due to PNC interactions within the nucleus will show up in atomic PNC experiments as a difference, typically of several percent, in the PNC transition amplitude on different hyperfine components of the atomic transition.

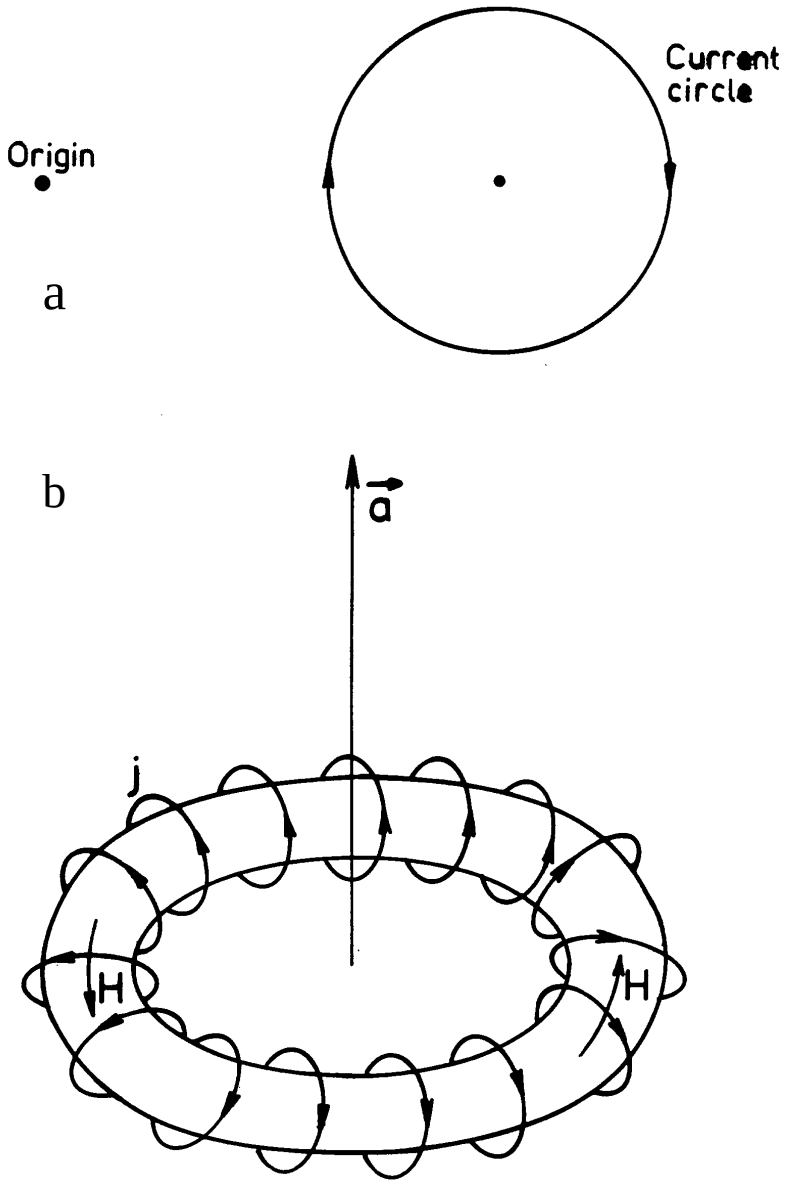

Fig. 3. The simplest systems with non-vanishing anapole moment (after Ref. [26]). a. A current loop displaced from the origin; b. A toroidal winding which can be thought of as a succession of such loops.

A simplified schematic of the Boulder experimental arrangement [10] is shown in Fig. 4. An atomic beam of Cs is produced in a multi-effusor array source. Along their way, atoms encounter diode laser beams 1 and 2 which optically pump them into a single desired Zeeman component of a single hyperfine state (F,m). Optical pumping is carried out in the presence of a y-directed magnetic field. As atoms continue downstream, the direction of this field is adiabatically rotated into the z-direction. The z-polarized atoms

then enter the main interaction region where they interact with an x-directed electric field (typ. 500 V/cm) and extremely intense elliptically-polarized standing-wave light tuned to the forbidden $6S_{1/2} \rightarrow 7S_{1/2}$ transition at 540 nm (Fig. 5). The standing wave is produced in a state-of-the-art power build-up cavity (finesse 100,000) and the circulating light power is about 2.5 kW. After a Cs atom is excited into the $7S_{1/2}$ state, it cascades back via the 6P states and has a probability >60 % to end up in a previously emptied hyperfine sublevel of the $6S_{1/2}$ state. This repopulation is detected about 10 cm downstream by a third diode laser beam. The frequency of this detection laser is tuned to a cycling transition, allowing more than one fluorescence photon per each absorption event in the main interaction region (typ. 100 to 240 depending on the hyperfine transition under investigation). Fluorescence is detected with a large-area silicon photodiode positioned directly below the atomic beam. This technique constitutes a low-noise signal amplifier. The signal detected by this apparatus is proportional to the transition rate in the main interaction region:

$$\begin{aligned} \left|A_E + A_{PNC}\right|^2 \cong\ & \beta^2 E_x^2 \varepsilon_z^2 \left[C_1(F, m, F', m')\right] + \\ & 2\beta E_x \varepsilon_z \cdot 2p\,\mathrm{Im}(\varepsilon_x)\,\mathrm{Im}(E1_{PNC})\left[C_2(F, m, F', m')\right] \end{aligned} \quad , \qquad (2)$$

where β is the vector Stark-transition polarizability, E_x is the dc electric field in the interaction region, ε_i are the components of the light polarization, $p=\pm 1$ is the handedness of the elliptical light polarization, $E1_{PNC}$ is the parity-violating electric dipole amplitude, and $C_{1,2}$ are combinations of the Clebsch-Gordan coefficients tabulated in [28]. This transition rate corresponds to a probability of about $5 \cdot 10^{-3}$ for an atom in the atomic beam to undergo the 6S→7S transition; the statistical fluctuations in the number of these atoms is the principal source of noise in this experiment. The form of Eq. (2) clearly illustrates the Stark-PNC interference nature of the measurement. Under typical conditions the second, PNC-dependent term in Eq. (2) constituted $\sim 6 \cdot 10^{-6}$ of the leading first term. Crucial to the success of the experiment are numerous built-in reversals (5 in all) which distinguish the real PNC effect from potential spurious effects. Such effects can arise from the apparatus imperfections and the presence of the M1 component of the transition

amplitude (the effect of the latter is significantly reduced since $A_{M1} \propto \vec{k} \times \vec{\varepsilon}$, and thus vanishes for a standing wave where $\langle \vec{k} \rangle = 0$). The PNC measurements in Cs performed up to now are summarized in Fig. 6. This figure illustrates remarkable consistency of various measurements performed over the years by the Paris and Boulder groups, the significant progress achieved, and the unambiguous discovery of a difference in the PNC effects for different hyperfine transitions in the latest experiment.

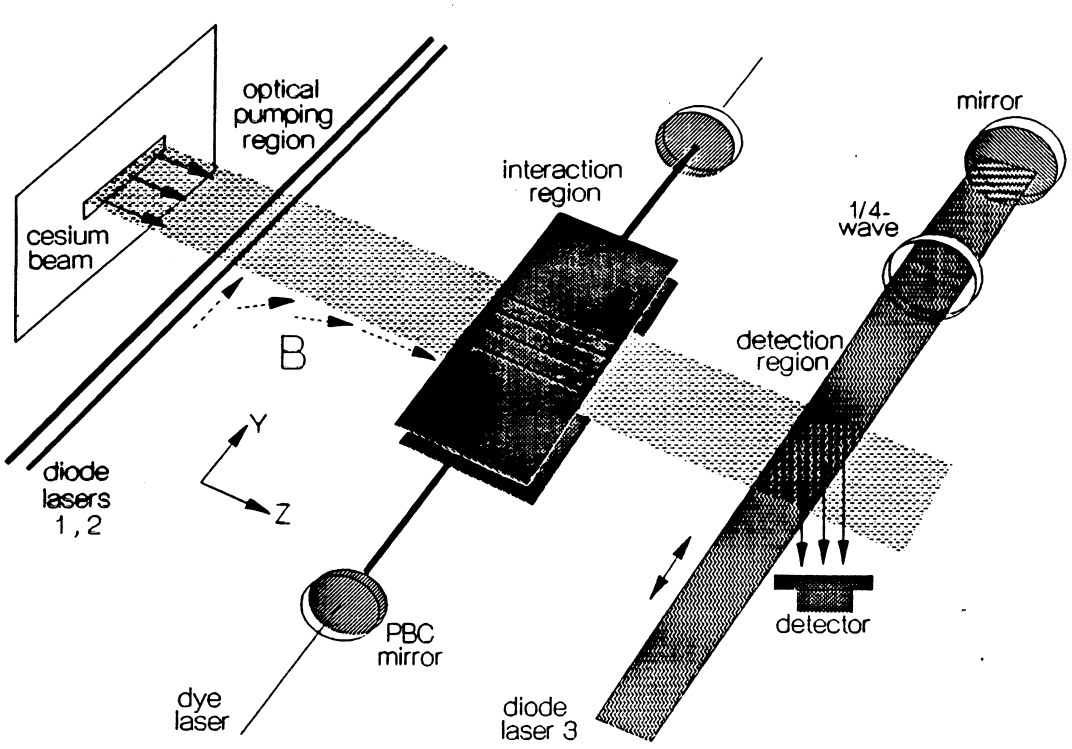

Fig. 4. A simplified schematic of the Boulder Cs experiment (From Ref 10).

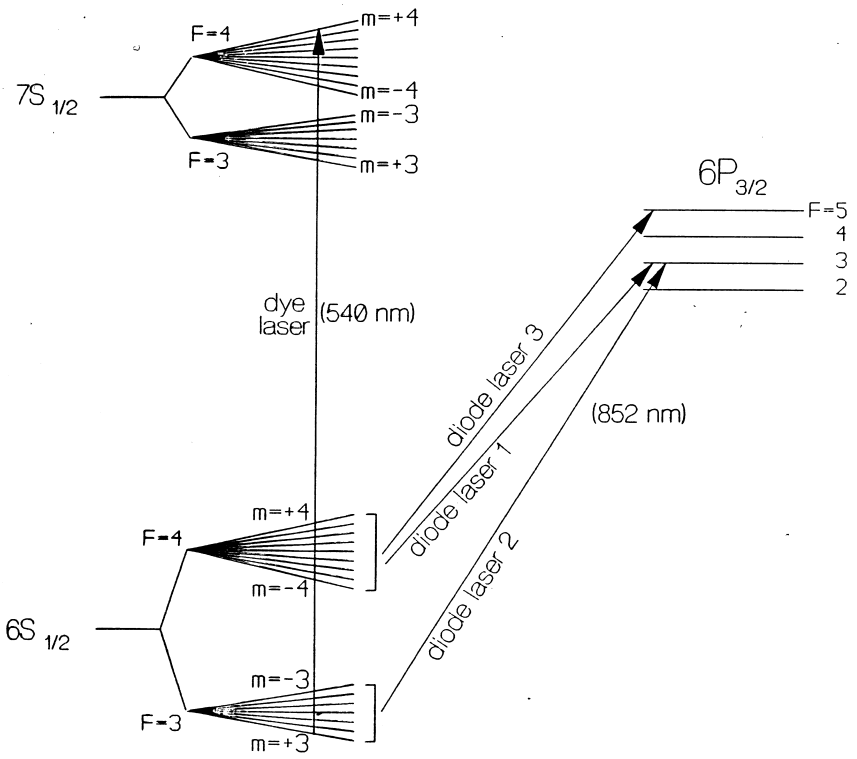

Fig. 5. Cs energy levels relevant to the PNC experiments and laser-induced transitions employed in the Boulder experiment [10].

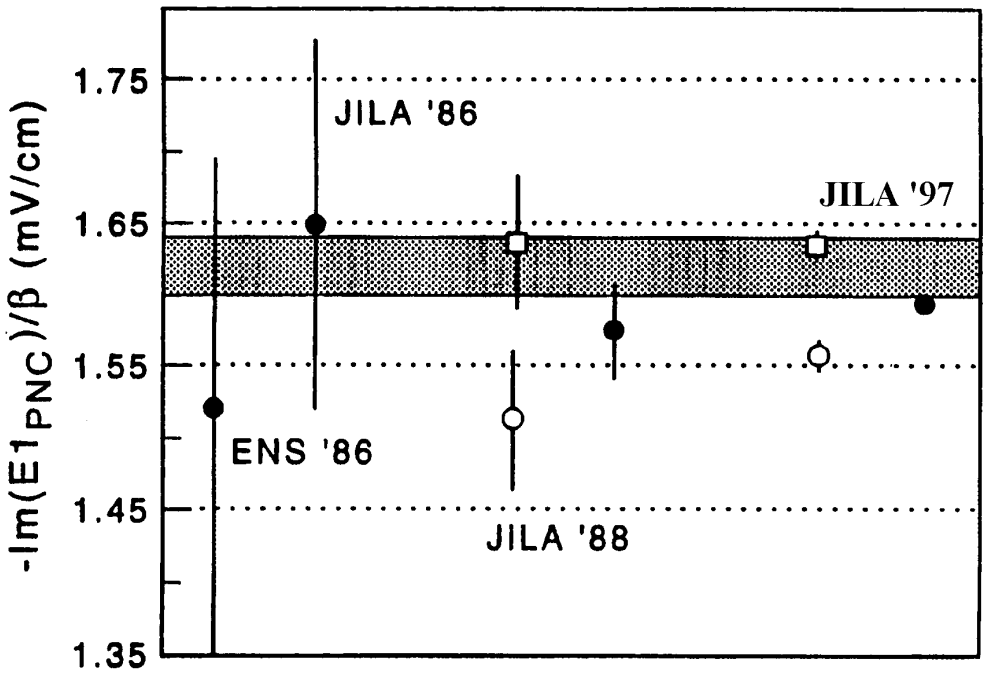

Fig. 6. Summary of the PNC results (adapted from Ref. 10). ENS: Ecole Normale Superieure, Paris; JILA: Joint Institute for Laboratory Astrophysics, Boulder. The squares: the 4-3 hyperfine transition; the open circles: the 3-4 transition; solid circles: averages over hyperfine transitions. The band: the standard model prediction for average. The width of the band represents $\pm 1\sigma$ uncertainty dominated by atomic theory.

Other ongoing Stark-PNC interference experiments

The Paris Cs experiment. The Paris group is continuing its efforts aimed at an improved measurement of PNC in the Cs 6S→7S transition [29]. In contrast to the Boulder group, they use a Cs vapor cell, rather than a beam. In their method, the forbidden transition is excited by a short (15 ns) linearly-polarized pump laser pulse in the presence of a longitudinal electric field. The upper state of the transition is detected on a time scale shorter than the lifetime of the 7S state (48 ns) by a probe laser pulse tuned to the $7S \rightarrow 6P_{3/2}$ transition. The use of stimulated emission for detection eliminates, in a way different from that of the Boulder group, the usual inefficiencies associated with fluorescence detection. The Stark-PNC interference is detected through the dependence of the gain on the relative orientations of the pump and probe polarizations $\boldsymbol{\varepsilon}_{pump}$ and $\boldsymbol{\varepsilon}_{probe}$ according to a pseudoscalar correlation

$\beta \cdot \mathrm{Im}E1_{\mathrm{PNC}}[\boldsymbol{\varepsilon}_{\mathrm{pump}} \cdot \boldsymbol{\varepsilon}_{\mathrm{probe}}][\boldsymbol{E} \cdot (\boldsymbol{\varepsilon}_{\mathrm{pump}} \times \boldsymbol{\varepsilon}_{\mathrm{probe}})]$, where $\boldsymbol{E}$ is the electric field. If the optical density of atoms in the 7S state is sufficiently high, the PNC-induced asymmetry can be amplified via nonlinear interaction of the probe beam with the atoms. This circumstance is used by the Paris group to optimize the signal-to-noise ratio of their experiment. Currently, the statistical sensitivity of their apparatus would allow a 1 % measurement of the PNC asymmetry with the same data accumulation time as their previous PNC measurement. The work is continuing on the analysis and elimination of all possible sources of systematics, many of them specific to this new method of PNC detection [15].

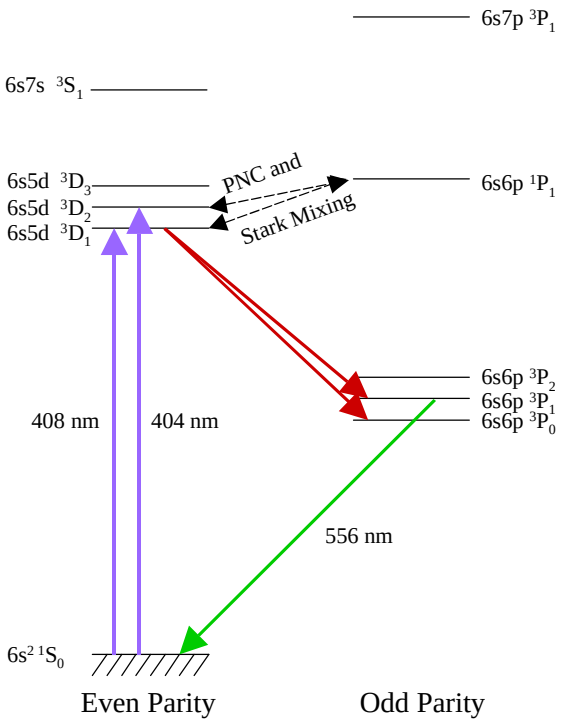

Fig. 7. Low-lying energy levels of Yb.

Stark-PNC interference experiments with Yb. A proposal to measure PNC in the ytterbium $6s^2\ ^1S_0 \rightarrow 6s5d\ ^3D_1$ transition (Fig. 7) was put forward by D. DeMille [30]. This transition has a highly-suppressed M1 amplitude and a moderately sized Stark-induced amplitude, allowing one to use the Stark interference technique. What makes this transition attractive is that the PNC amplitude should be more than 100 times larger than in Cs [28,31]. This enhancement is primarily due to the fact that the $^3D_1$ state lies

very close ($\Delta E \cong 600$ cm^{-1}) to a level of opposite parity ($^1P_1$) which is nominally of the 6s6p configuration, but is strongly configuration-mixed with 5d6p. Configuration mixing gives rise to large weak interaction mixing between $^1P_1$ and $^3D_1$ (from the 5d6p $^1P_1$ component), and, at the same time, to a strong E1 amplitude to the ground state (from the 6s6p $^1P_1$ component). It is worthwhile to emphasize an important difference in the reliability of the prediction of a large PNC effect in Yb compared to other rare earth atoms, particularly Dy, where the PNC amplitude was found to be much smaller than predicted (see below). Yb, with 14 4f-electrons, has a completely filled 4f-shell in its low-lying energy states. Therefore, the spectrum of Yb is considerably simpler than that of other rare earth atoms with fewer 4f-electrons and is much more amenable to reliable theoretical analysis. The uncertainty in the calculated PNC amplitude is estimated at about 20%. Yb (Z=70) has seven stable isotopes between A=168 and 176, so an isotopic PNC comparison can be made. Two of the isotopes have non-zero nuclear spin (^{171}Yb, I=1/2 and ^{173}Yb, I=5/2) and can be used to measure the anapole moments. A calculation of nuclear-spin dependent PNC amplitudes in Yb isotopes has been recently performed in [32]. The anapole moment measurements can in principle be performed on both the $^1S_0 \rightarrow {}^3D_1$ and $^1S_0 \rightarrow {}^3D_2$ transitions. Compared to $^3D_1$, the $^3D_2$ state is about two times closer to $^1P_1$. PNC mixing between $^3D_2$ and $^1P_1$ occurs only due to nuclear spin-dependent interactions ($\Delta J=1$); thus, the nuclear-spin dependent PNC effect will be the only source of PNC in the $^1S_0 \rightarrow {}^3D_2$ transition, rather than a relatively small correction to the dominant nuclear spin-independent amplitude as in the case of $^1S_0 \rightarrow {}^3D_1$ [33,32]. A disadvantage of this transition is that the Stark-PNC interference experiment has to be performed in the presence of a relatively large $E2$ amplitude (see below) potentially leading to systematic effects. These effects and optimal design of a PNC experiment are the subject of an ongoing analysis.

Before the actual PNC experiments begin, it is important to obtain experimental information on various atomic parameters. This information is essential for demonstrating our understanding of the system, for optimizing the PNC experiment, and for reducing possible systematic uncertainties. Measurement of the lifetimes of the 6s5d $^3D_{1,2}$ states (and twenty other states in Yb) was reported in [34]. Measurements of the hyperfine structure, isotope and Stark shifts, and the Stark-induced and $E2$ amplitudes of

the $6s^2\,{}^1S_0 \rightarrow 6s5d\,{}^3D_{1,2}$ transitions are now complete, and a measurement of the $M1$ amplitude is in progress [35]. Fig. 8. shows an experimental recording of the Stark-induced transition at 408 nm and the decomposition of the trace into contributions from various isotopic and hyperfine components. The magnitude of the vector transition polarizability of the ${}^1S_0 \rightarrow {}^3D_1$ transition was measured to be $|\beta| = 2.2(3)\cdot 10^{-8}\ \dfrac{ea_o}{V/cm}$. For the ${}^1S_0 \rightarrow {}^3D_2$ transition, it is the tensor polarizability γ that leads to the Stark-induced transition. This was measured to be of the magnitude $|\gamma| = 4.1(2)\cdot 10^{-8}\ \dfrac{ea_o}{V/cm}$. For this transition, the fluorescence signal is still observable when the electric field is turned off. This is due to the contribution of the $E2$ amplitude which was thus measured to be $\left|\left\langle {}^3D_2 \middle\| E2 \middle\| {}^1S_0 \right\rangle\right| = 1.45(7)\ ea_0^2$.

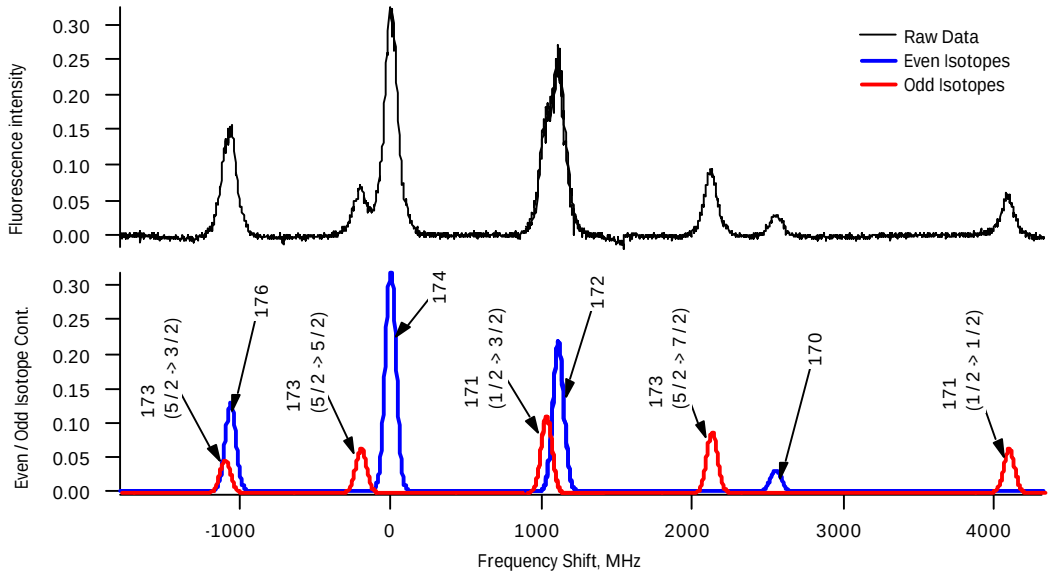

Fig. 8. Observation of the Stark-induced $6s^2\,{}^1S_0 \longrightarrow 5d6s\,{}^3D_1$ transition in Yb. Atoms in an atomic beam in a 45 kV/cm electric field are excited with light at 408 nm. Fluorescence is observed at 556 nm from the cascade decay through the $6s6p\,{}^3P_1$ state.

Upon the completion of the $M1$ measurement for the ${}^1S_0 \rightarrow {}^3D_1$ transition, an atomic beam PNC measurement on this transition will commence. In the meantime, we are also exploring possibilities of conducting a PNC experiment in a vapor cell, which would have the advantage of a higher counting rate than in an atomic beam experiment.

The idea is to accumulate atoms excited to the $^3D_1$ state in the metastable 6s6p $^3P_0$ state, where the $^3D_1$ state decays with a 70 % probability. The population of $^3P_0$ can be then probed by measuring absorption of laser light tuned to the 648.9 nm transition to the 6s7s $^3S_1$ state. For an ytterbium PNC experiment in a vapor cell to be advantageous, it is important that the metastable $^3P_0$ state be long lived with respect to collisional quenching. The energy level structure of low-lying states in Yb is similar to that of Hg, where collisional de-excitation cross sections for the 6s6p ^3P_J metastable states are small [36]. We are measuring the collisional de-excitation cross sections of $^3P_0$ with respect to various noble buffer gases and the pressure broadening and shift of the 648.9 nm line to determine the most favorable gas for use in the PNC experiment. For these measurements, we use a resistively heated stainless steel vapor cell with a tantalum liner. The $^3P_0$ state is populated by exciting Yb atoms from the ground state to the 6s7p $^3P_1$ state with a pulsed 262 nm pump beam (produced by a frequency-doubled Excimer-pumped dye laser), which subsequently populates $^3P_0$ via cascade decay. The population of $^3P_0$ is continuously probed by measuring absorption of light from an external cavity diode laser tuned to the 648.9 nm transition. The diode laser is tuned to resonance by splitting part of its output into a Yb hollow cathode lamp and observing the amplitude of the optogalvanic signal. By varying the temperature of the cell (T_{cell}=700-1200 K, which corresponds to Yb densities of 10^{11}-10^{15} cm^{-3}) and the pressure of the buffer gas, we are able to determine the Yb-Yb cross sections along with the Yb-buffer gas cross sections.

On the whole, Yb appears to be one of the most promising atoms for future PNC measurements.

The Dy experiment. Measurement of PNC in nearly-degenerate levels of opposite parity in atomic dysprosium (Z=66) has been driven by the possibility of making such a measurement at a precision orders of magnitude better than so far achieved in other elements. This possibility arises from the unusually small, essentially zero, energy splitting [23,37].

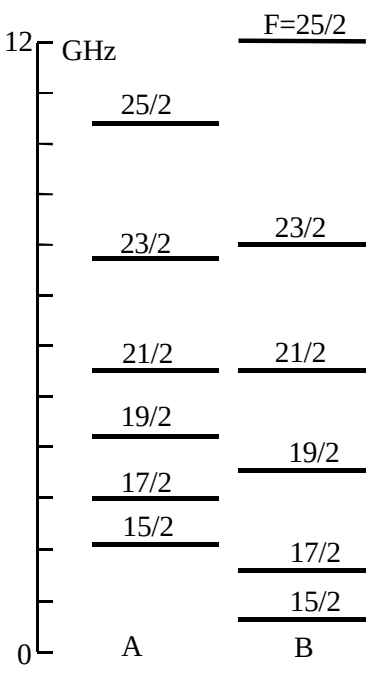

Fig. 9. Hyperfine structure of levels A and B of ^{163}Dy.

The nearly-degenerate levels (A, even parity, and B, odd parity) both have angular momentum J=10 and lie 19797.96 cm^{-1} above the ground level (J=8). (The overall known level structure of atomic Dy is tabulated in [38]) Dysprosium has stable isotopes with both even and odd neutron numbers ranging from A=156 to A=164. The precise magnitude of the energy splitting between A and B [39] is that typically associated with hyperfine (HF) and isotope shifts (IS) and varies greatly among the various HF and IS components. For the even isotopes (which have nuclear spin I=0, and no hyperfine structure) the splitting ranges from 235 MHz for ^{162}Dy to 4200 MHz for ^{156}Dy. The two odd isotopes (^{161}Dy and ^{163}Dy) both have nuclear spin I = 5/2. Fig. 9 shows the hyperfine structure of levels A and B in ^{163}Dy. The hyperfine components with F=21/2 of ^{163}Dy are the closest pair, with a separation of only 3.1 MHz (This is 300 times less than the Lamb shift between the $2S_{1/2}$ and $2P_{1/2}$ states in hydrogen!). This pair of levels in ^{163}Dy is used in the current search for PNC.

Our approach in the PNC experiment is to observe Stark-induced quantum beats between levels A and B and to search for interference between the Stark amplitude and the much smaller PNC matrix element between the two levels. A magnetic field is applied to bring Zeeman sublevels of A and B with the same m_F nearly to crossing, thus enhancing the PNC mixing between them. An electric field is applied parallel to the magnetic field to induce significant quantum beats. The Stark and PNC amplitudes have $\pi/2$ relative phase and do not interfere in a DC electric field. In order to alter the phases and to produce interference between these two amplitudes, the electric field is harmonically oscillating (f=100 kHz). A somewhat analogous (non-adiabatic E-field switching) scheme of PNC detection was previously proposed for the 2s-2p system in hydrogen [40]. In the recently completed PNC measurement [41] using pulsed lasers, quantum beats were observed by populating level A instantaneously at time t=0, transferring the population to B with an electric field 'π-pulse', and probing the time-

dependence of the population of A which arises from the harmonic electric field. In this arrangement, we take advantage of the long lifetime (τ>200 μsec) of the odd-parity state. Level A was populated by two-step excitation from the ground state via an intermediate odd-parity level with J=9; the corresponding E1 transitions were induced by two consecutive laser pulses at 626 nm and 2614 nm. Population of A was measured by observing cascade fluorescence. The PNC effect manifests itself in a characteristic 'first harmonic' asymmetry of the fluorescence signal relative to the fundamental frequency of the applied electric field. The PNC asymmetry can, in principle, be extracted from each laser pulse, so this method is insensitive to the pulse-to-pulse fluctuations typical in the output power and spectrum of pulsed lasers. Using the predicted value of the weak interaction matrix element between A and B H_w=70(40) Hz [42], and the Stark amplitude and the lifetimes of the states measured in [43], we estimated the asymmetry under optimal experimental conditions to be very large: on the order of

$$\frac{H_W}{\sqrt{\Gamma_A \cdot \Gamma_B}} \approx 2\times10^{-2}. \qquad (3)$$

Here the Γ-factors are the effective widths of the states ($\Gamma_A=1/\tau_A$; τ_A=7.9 μsec; since B has a very long lifetime, τ_B>200 μsec, the effective width of B is determined by the length of the atomic beam apparatus, $(\tau_B)_{effective}\approx$200 μsec). This asymmetry changes sign with the overall applied magnetic field and with the residual level 'decrossing factor' Δ; it has the signature of the P-odd, T-even invariant $\dot{\mathbf{E}}\cdot(\mathbf{B}-\mathbf{B}_C)$, where the time derivative of the electric field reflects the fact that the PNC-Stark interference manifests itself in the time-dependence of the signal (and not in the steady-state transition amplitude), and $\mathbf{B}_c$ is the magnetic field required to produce an exact level crossing.

It is crucial that a precise PNC experiment be capable of controlling systematic effects. In our system, the availability of multiple field reversals which change the sign of the asymmetry leads to rejection of systematic effects from stray and nonreversing fields. In addition, the presence of spurious fields is detected and corrected for with numerous auxiliary measurements using the Dy atoms themselves. It is interesting to note that the magnitude of a stray or non-reversing electric field required to produce mixing as big as

the predicted PNC mixing is large: $\left|H_W / d\right| \approx 10\, mV/cm$. For these reasons, the systematic effects are well under control.

The experimental configuration is shown in Fig. 10. Dy beam was produced by an effusive oven source (T≈1500 K) with multi-slit nozzle array. A chopper wheel blocked oven light during fluorescence detection. A magnetic field brings Zeeman sublevels ($|A, F = 21/2, M_F\rangle$ and $|B, F = 21/2, M_F\rangle$) to near-crossing. After two consecutive laser pulses (626 nm and 2.6 μm) excite atoms to state A, a 17 V/cm, 3.1 μsec rectangular electric field pulse (π-pulse) transfers atoms from a given sublevel to the longer-lived state B ($|A, F = 21/2, M_F\rangle \rightarrow |B, F = 21/2, M_F\rangle$). The oscillating electric field (100 kHz, 4 V/cm) is then applied. Mirrors surrounding the interaction region and a light pipe collect light from cascade fluorescence of state A onto a photomultiplier tube.

The PNC results obtained in several experimental runs over a period of several months are summarized in Fig. 11. We find that the weak matrix element in Dy is:

$$|H_W| = 2.3 \pm 2.9(\text{stat.}) \pm 0.7(\text{syst.})\ \text{Hz}. \qquad (4)$$

The experimental uncertainty in the weak interaction matrix element is at least an order of magnitude smaller than in any other atomic PNC experiment. Our result is outside the range of the theoretical prediction of 70±40 Hz [42]. Theoretical efforts [44] aim at understanding the origin of this discrepancy.

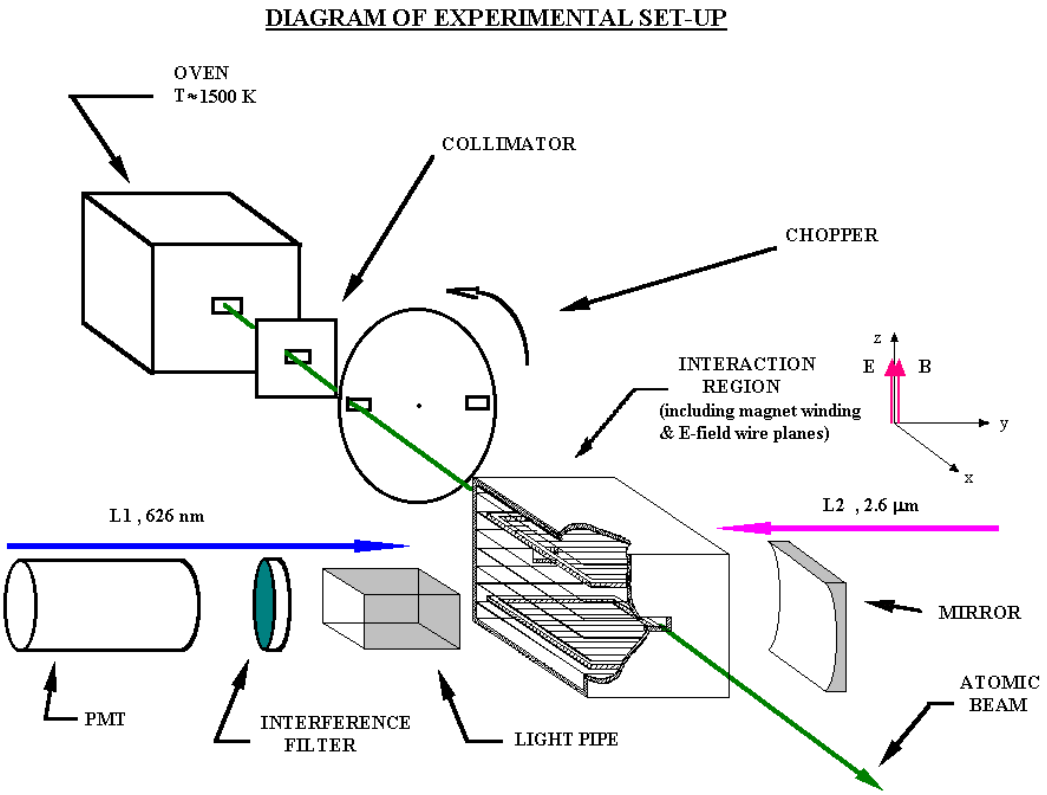

Fig. 10. Schematic view of the Dy PNC apparatus.

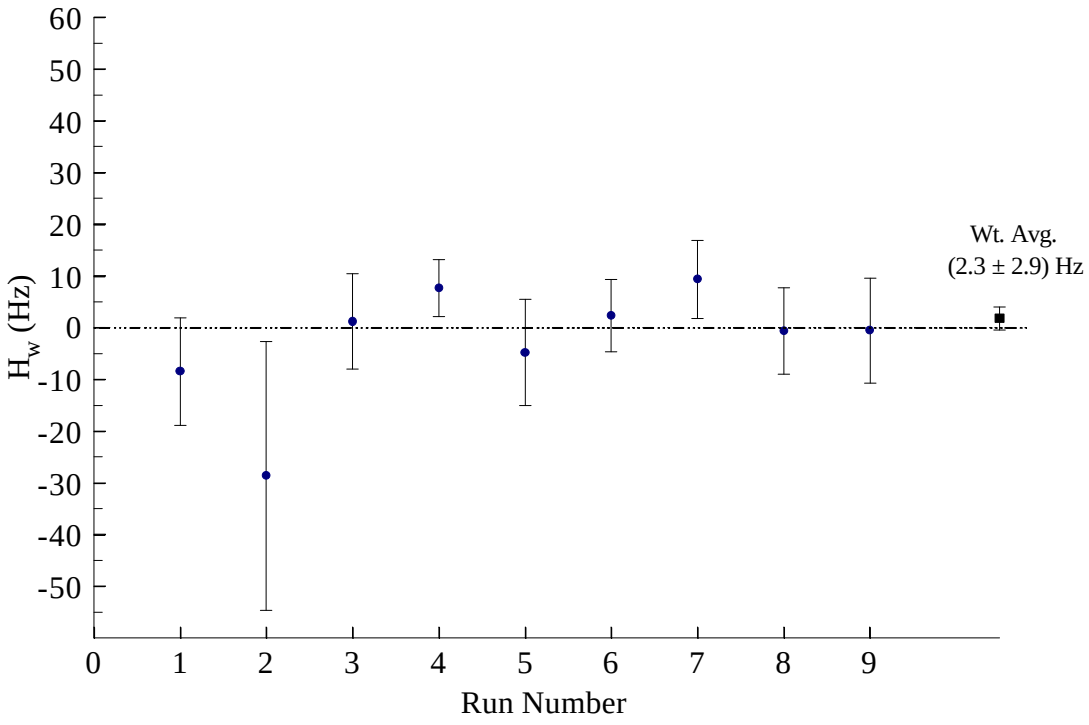

Fig. 11. Summary of the Dy PNC data.

The remarkable sensitivity of the Dy experiment to H_W is due in part to the unusual properties of Dy levels - the opposite parity states are close enough that a small magnetic field can bring them to crossing, and, in addition, both of these states have relatively long lifetimes. Unfortunately, the prospects of precision PNC measurements in Dy are uncertain because the weak matrix element turned out to be so small. To perform meaningful comparisons of PNC effects on different isotopic and hyperfine components, it will be necessary to measure PNC on each component at least to ~0.1%. The present upper limit on the PNC matrix element is about 5 Hz. We estimate, that with the improvements of the apparatus described below, it will be possible to achieve a sensitivity ~1 mHz. A PNC matrix element of 1 Hz is borderline and a smaller matrix element would make isotopic and hyperfine comparisons unreasonably difficult. At this point, we are interested in increasing the experimental sensitivity to a level where the PNC effect can be unambiguously determined.

The main feature of the new experiment is that, since it utilizes cw lasers instead of the pulsed lasers with 10 Hz repetition rate, it provides a ~100% duty cycle (instead of $\approx 10^{-4}$ in the pulsed experiment). Optical pumping of atoms into a single Zeeman sublevel can gain a factor of ~ 20 in signal. These features should give a statistical sensitivity of ~ 1 mHz in a month of data taking. A diagram of the population and probe transitions for the new PNC experiment in Dy is shown in Fig. 12. Population of the state B will be accomplished using three *E*1-transitions induced by diode lasers. The most attractive scheme involves three relatively strong transitions at 833 nm, 669 nm, and 1397 nm. Powerful single-mode diode lasers are commercially available for all three wavelengths. In this experiment, we use a weakly collimated atomic beam with collimation ratio ~1:10 which corresponds to a transverse Doppler width on the order of a hundred MHz. In order to efficiently transfer atoms in all velocity groups from the ground state to the state B, divergent laser beams (matching the divergence of the atomic beam) are used. This ensures that all transverse velocity groups of atoms interact with the laser light with comparable efficiency. In this arrangement, each atom traversing the laser beams 'sees' frequency-chirped light fields sweeping across their respective resonance frequencies. For a single transition with appropriate choice of laser parameters this corresponds to

"adiabatic fast passage" - a process leading to very efficient population transfer to the upper state (robust π-pulse). Using computer modeling, we have generalized this approach to the case of a multi-stage excitation [45], and found that a significant fraction of the ground state atoms can be transferred to the state B with rather modest diode laser power of a few mW for each laser.

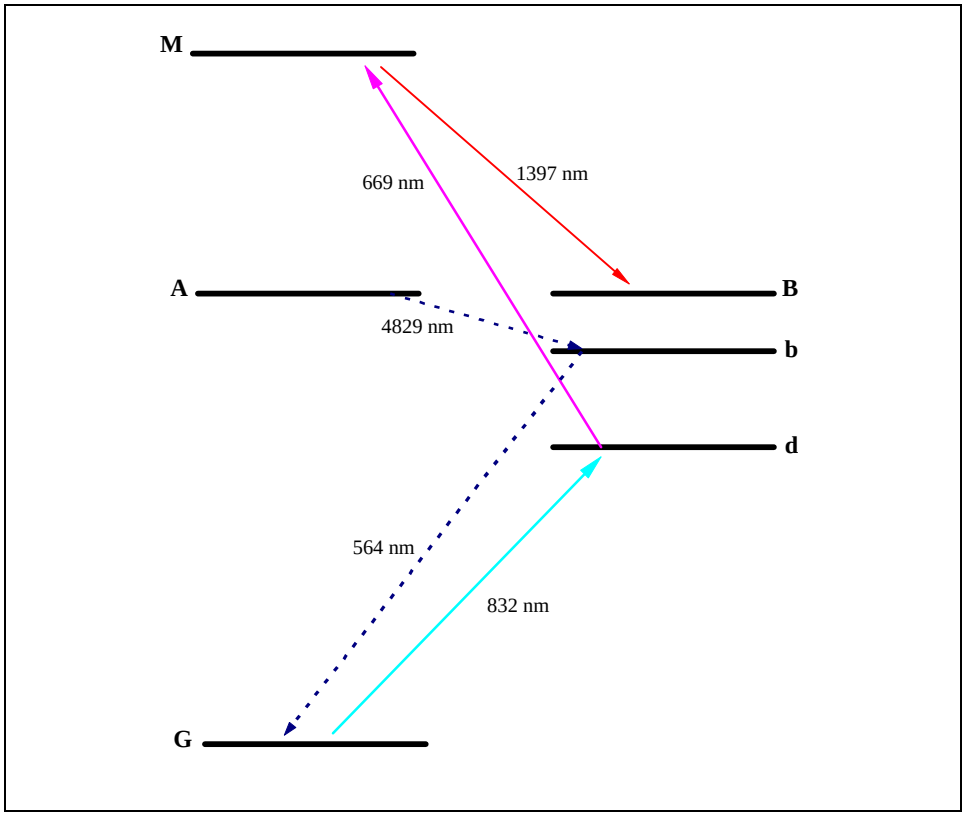

Fig. 12. Schemes for population of state B and detection of state A. Solid arrowheads: laser-induced transitions; dashed lines: spontaneous transitions.

New approaches to optical rotation

Search for enhanced optical rotation in Sm. Samarium was the first rare earth element considered for PNC experiments, beginning with theoretical work in 1986 [23,46]. From 1987-89, work was undertaken in Novosibirsk to find new levels suitable for parity-violating optical rotation studies [47]. Following this, PNC experiments at Oxford examined the proposal [46] and transitions involving the new levels found in Novosibirsk and have determined that none of these schemes produce an observable PNC effect, much less an enhancement [48,49,50]. However, more extensive and precise spectroscopic knowledge, including location of new levels, may reveal new possibilities for PNC

research. The point is that for a successful PNC experiment, one needs a right combination of several atomic matrix elements, including large PNC mixing between the closely lying states, a suitable $M1$ amplitude from the ground state to one of them, and a large $E1$ amplitude from the ground state to the other. Spectroscopy in samarium was carried out to this end in [51] where scalar and tensor electric polarizabilities were measured, and in [52,53] with measurement of hyperfine structure, g values and tensor polarizabilities of certain samarium states. A systematic study of lifetimes and tensor polarizabilities of the low-lying odd parity states was carried out at Berkeley [54]. This will be followed by a search for more new levels in Sm.

Application of electromagnetically-induced transparency to optical rotation. It has been recognized for some time that the methods of nonlinear spectroscopy may be useful in atomic PNC experiments (see e.g. the description of the new Paris experiment above and Ref. 55). In a new approach pursued by the Seattle group [56], they are attempting to use the technique of electromagnetically-induced transparency (EIT) [57] to address the problems of the traditional optical rotation PNC experiments, namely, the problem of detailed understanding of a complicated spectral lineshape, and the absence of reversals that would help distinguish a true PNC rotation from systematics. The energy level diagram relevant to the Seattle EIT work is shown in Fig. 13. As in their previous PNC experiments, optical rotation is detected with a probe laser beam tuned to the $6P_{1/2} \rightarrow 6P_{3/2}$ M1/E2 transition at 1.28 μm. Now, however, there is a second, counter-propagating pump laser beam present whose frequency is tuned to an the $6P_{3/2} \rightarrow 7S_{1/2}$ fully allowed transition. The presence of this pump beam modifies the effective refractive index "seen" by the probe beam in a drastic way. This is because the dynamical Stark effect due to the pump light splits the $6P_{3/2}$ state into an Autler-Townes doublet, thus changing the refractive index near the center of the probe line. The main advantages of using this scheme for a PNC measurement are that the optical rotation lineshapes are now Doppler-free and can be turned on and off by simply modulating the pump beam intensity. This should considerably simplify subtraction of background rotations and will also allow investigation of individual isotopic and hyperfine components of the transitions that are no longer blended by the Doppler broadening. A serious drawback of the method is related to thermal population of atoms in the $6P_{3/2}$ state leading to absorption of the pump

beam. This limits the maximum usable vapor density at a level some three orders of magnitude lower than in the previous Tl PNC experiment [58]. Nevertheless, the

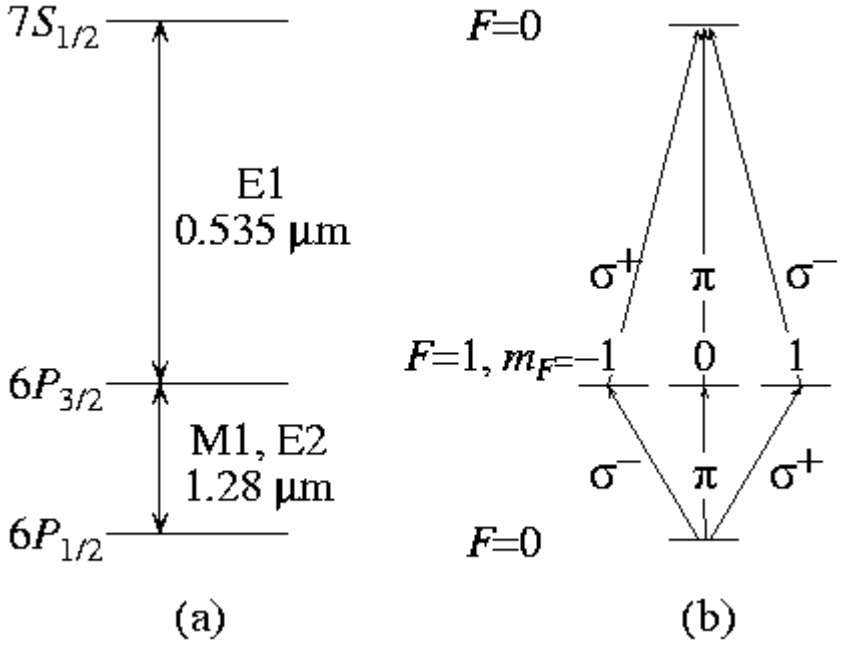

Fig. 13 (adapted from Ref. 56) Energy levels participating in EIT:
Fig.1 (a) The three level system studied in Tl. (b) transitions among Zeeman substates for the (F=0 → F'=1 → F''=0) EIT channel.

technique remains sensitive enough to allow a statistically-limited detection of PNC rotation at a 0.5 % level in a 2 hr measurement [56]. Various systematic effects, including those due to residual circular polarization of the pump beam ("chiral corruption") and ways to eliminate them are currently under investigation by the Seattle group.

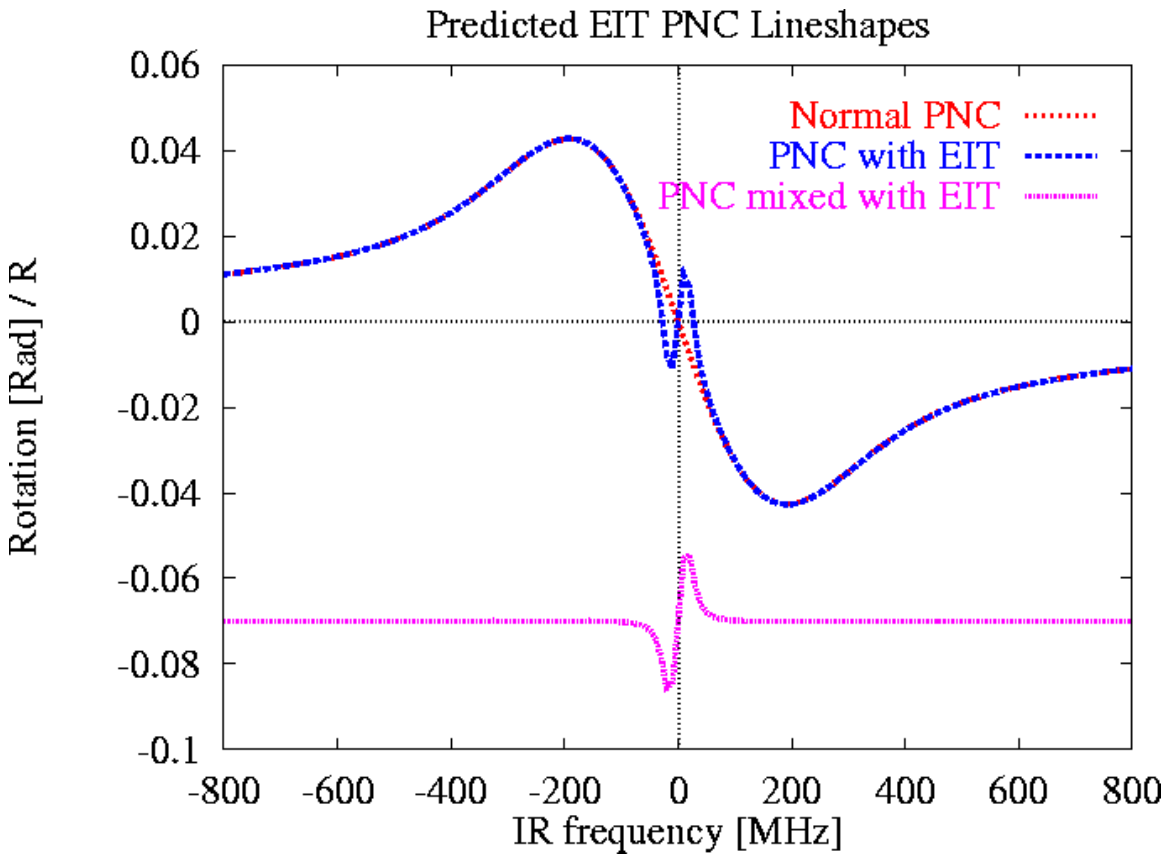

Fig. 14. (From A. Cronin's web page: www.phys.washington.edu/~cronin/). R=Im($E1_{PNC}/M1$)≈10^{-7}. IR frequency refers to the 1.28 μm probe transition. The lowest trace may be obtained in experiment by chopping the pump beam and using the lock-in detection.

E2-E1$_{PNC}$ interference, parity-violating light-shifts and single ion PNC experiments

An interesting approach to atomic PNC, which is radically different from all other PNC experiments, involving measurements on just a single trapped ion, is being pursued by the Seattle group [59]. To illustrate the principle of this experiment, we first consider the lowest energy levels of the Ba^+ ion used in the current experiments (Fig. 15). The ground $6S_{1/2}$ state has a PNC-induced admixture of the $nP_{1/2}$ states (the contact weak interaction only mixes $S_{1/2}$ and $P_{1/2}$ states), which leads to an electric dipole component of the $E2$ (quadrupole) $6S_{1/2}\rightarrow 5D_{3/2}$ transition: $E1_{PNC}\approx 2\cdot 10^{-11} e\cdot a_0$. This is similar to the PNC-induced amplitude in Cs, and can be calculated as accurately, or even better [59].

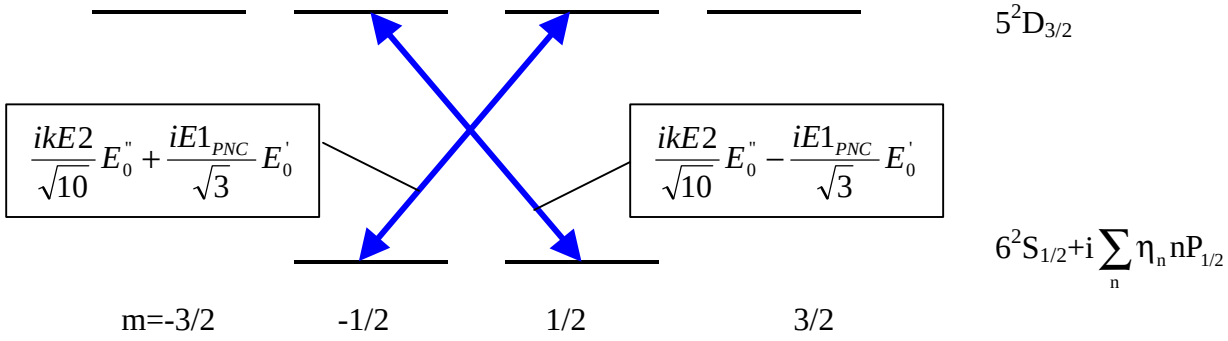

Fig. 15. Lowest energy levels of the Ba^+ ion. The PNC interaction mixes higher-lying $P_{1/2}$ states to the ground state. Arrows indicate the relevant $E2/E1_{PNC}$ transitions, whose amplitudes are given in the corresponding boxes.

Now suppose that the ion is positioned at the origin, where it is being irradiated by two standing light waves, both of which are resonant with the $6^2S_{1/2} \rightarrow 5^2D_{3/2}$ frequency, with electric fields:

$$\mathbf{E}' = \hat{x}E_0^{'}\cos(kz); \quad \mathbf{E}'' = i\hat{z}E_0^{"}\sin(kx) \tag{5}$$

The first of these waves is optimized to drive the $E1_{PNC}$ amplitude by having an electric field node at the ion's position. Since the polarization of this wave is along x, it drives the $\Delta m=\pm 1$ transitions. The second wave has zero electric field amplitude at the origin, but the maximum gradient. This is optimal for driving the $E2$ amplitude. The relevant amplitudes with appropriate Clebsch-Gordan coefficients included are shown in Fig. 15 (it turns out that the transitions to the $m=\pm 3/2$ sublevels are irrelevant since they are shifted out of resonance by the off-resonant AC Stark-effect caused by the strong field **E**'). It is clear that whereas the two amplitudes, $E2$ and $E1_{PNC}$, interfere constructively for the $\Delta m=1$ transition, they interfere destructively for the case of $\Delta m=-1$. The interference can be detected by measuring a difference in the light shift for the $m=\pm 1/2$ sublevels. In the presence of the $E2$ field **E**", each of the ground state $m=\pm 1/2$ sublevels is split into an Autler-Townes doublet, the components of which are shifted from the unperturbed energy by $\pm\Delta\omega^{quad} \approx 10^{-4} ea_0 E_0^{"}/\hbar$ [59]. Using appropriate adiabatic turn-on procedure

for the field **E**", the ion can be placed into a chosen (e.g. lower-energy) component of the doublet. The $E2$-$E1_{PNC}$ interference leads to a difference in the shift for m=1/2 and –1/2: $\Delta\omega^{PNC} \approx 10^{-11} e a_0 E_0^{'} / \hbar$. This difference can be detected by e.g. measuring the energy between m=1/2 and –1/2 in a small bias magnetic field in the z-direction using radio-frequency spectroscopy.

The Seattle experiment utilizes well-developed techniques of ion trapping and cooling. An ion is first captured in an RF trap in the center of a ring electrode (~500 μm; potential well depth ≈50 eV; trap frequency ≈25 MHz; characteristic frequency of oscillation in the trap ≈5 MHz). Laser cooling is then applied to reduce the ion's temperature to the Doppler limit ~1 mK. This localizes the ion in a region ~0.1 μm, i.e. considerably smaller than the 2.05 μm wavelength of the $6^2S_{1/2} \rightarrow 5^2D_{3/2}$ quadrupole/PNC transition. Laser cooling is performed on the 493 nm $6^2S_{1/2} \rightarrow 6^2P_{1/2}$ $E1$ transition. Since atoms excited to the $6^2P_{1/2}$ state can also decay to the $5^2D_{3/2}$ state, it is necessary to use another "clean-up" laser beam at 649 nm to pump the atoms back into $6^2P_{1/2}$. Once the ion has been trapped and cooled, it can remain like that for several hours. After cooling has been accomplished, the cooling lasers are turned off and the fields $\mathbf{E}^{'}$ and $\mathbf{E}^{''}$ are turned on for up to ~50 sec – the lifetime of the $5^2D_{3/2}$ state. At this point it would seem desirable to maintain the amplitude of the field $\mathbf{E}^{'}$ as high as possible to increase the value of the PNC-induced light shift. It turns out, however, that non-resonant excitation processes coupled with spontaneous decay effectively shorten the $5^2D_{3/2}$ lifetime leading to deterioration of signal-to-noise. The optimum value of the light field amplitude is found to be $E_0^{'} \sim 10^4$ V/cm (leading to $\left|\Delta\omega^{PNC}\right| / 2\pi \approx 0.4$ Hz). Note that such high amplitude of the light field is relatively easy to achieve in this experiment because the laser beam can be tightly focused at the location of the ion. While the fields $\mathbf{E}^{'}$ and $\mathbf{E}^{''}$ are on, the energy difference between m=1/2 and –1/2 is measured in the following manner. A bias magnetic field $\sim 10^{-4}$ Gs is applied in the z-direction causing the Larmor frequency (Zeeman splitting) to be ~100 Hz (The magnitude of the quadrupole field is chosen $E_0^{''} \sim 10^{-2} E_0^{'}$, so the Larmor frequency is a small fraction of the quadrupole light shift. This is done in order to avoid possible systematic effects related to laser mistuning). To measure the Larmor frequency, a transverse resonantly oscillating magnetic field is

applied. The transition between the originally populated m-level and the initially empty m-level induced by the oscillating magnetic field is monitored using a shelving technique in which (yet another) circularly-polarized laser beam tuned to the $6^2S_{1/2} \rightarrow 5^2D_{5/2}$ $E2$ transition (1.76 μm) which selectively couples to the originally empty m-sublevel. This is how it works. At the end of the measurement cycle, the cooling and clean-up beams are turned on. If the ion at this point is in any of the sublevels of the $6^2S_{1/2}$, one will see fluorescence photons (mostly at 493 nm). If, however, the ion made the transition to the m-sublevel coupled to the shelving light field and further made the transition to the $5^2D_{5/2}$ shelf ($\tau \approx 1$ sec), the fluorescence will be absent for the lifetime of the shelf. In principle, this method is ~100 % efficient.

The statistical accuracy of this method of measuring PNC can be estimated as:

$$\frac{E1_{PNC}}{\delta E1_{PNC}} \cong \frac{E1_{PNC} E_0^{'}}{\hbar} f \sqrt{N\tau t} \,, \qquad (6)$$

where f is the efficiency factor, τ is the coherence time determined by the $5^2D_{3/2}$ decay, t is the overall time available for the measurement, and N=1 is the number of ions. With f=0.2, $\boldsymbol{E}1_{PNC}$ can in principle be measured to 1 part in a 1000 in about a day. From Eq. (4), it is clear that the statistical power of this method stems from a possibility to create large electric field at the location of the ion and from the long inherent coherence time associated with the $6^2S_{1/2} \rightarrow 5^2D_{3/2}$ transition. These advantages allow a competitive sensitivity to PNC, despite the huge loss taken in the number of atoms involved in the measurement as compared to more traditional methods.

Various sources of systematics have been analyzed by the Seattle group. They find that the false PNC shifts arise only in the presence of multiple imperfections of the apparatus, and thus can be controlled at a level much smaller than the true PNC shift. One class of systematic effects is related to the off-resonant dipole shifts due to the field **E'**. A residual circular polarization of this field will cause an m-dependence in the light shift, potentially much greater than the PNC shift. This effect is considerably mitigated, however, because the spurious shift, in contrast to the PNC shift, does not show sharp changes with laser tuning about the $6^2S_{1/2} \rightarrow 5^2D_{3/2}$ transition. The geometry of the

experiment can also be chosen in such a way that the PNC precession axis is perpendicular to the laser beam axis, leading to an additional suppression of the systematic effect [60].

As was mentioned earlier, Ba^+ is an attractive object for PNC experiments, both because the PNC amplitude here is relatively large, and because accurate atomic calculations are possible. Additional advantages of Ba stem from the fact that it has nine stable isotopes with vastly different number of neutrons ($\Delta N=8$). This may prove to be useful for a systematic investigation of PNC in an isotopic chain. Note that only trace amounts of material are necessary for this type of experiments. An analogous measurement could also be carried out in a much heavier radioactive ion $^{226}Ra^+$ ($\tau_{1/2}$=1600 y), where PNC effect is several times larger.

As a final note in this section, we mention a proposal [61] to use the PNC-shift in NMR frequency of atoms irradiated by laser light for measurements of the nuclear anapole moments.

Ideas for future experiments

Trapped neutral atoms. Similar to the case of ions, recent spectacular developments in laser trapping and cooling of neutrals may find application in the PNC experiments. For example, trapping allows one to work with a relatively small number of atoms, so radioactive samples can be used. This may allow carrying out isotopic comparisons for Cs [62], where there is only one stable isotope (^{133}Cs), but there is a range of relatively long-lived ($\tau_{1/2}$>9 min) radioactive isotopes between ^{125}Cs and ^{139}Cs. Work is also in progress on the study of the heaviest alkali atom, Fr (Z=87) [63] with one of the ultimate goals being a PNC measurement.

Relativistic ions. It has long been a dream of atomic physicists to measure PNC in hydrogen (for a review of hydrogen experiments, see [64]), or a hydrogenic system. It appears that recent developments in relativistic ion colliders, high-brightness ion sources, and laser cooling methods of ions in storage rings, may open such a possibility for relatively light (Z~10) hydrogenic ions [65]. Due to their simple atomic structure, high precision theoretical calculations can be carried out in these ions. In addition, neutron distribution uncertainties will not present a serious problem in relatively light ions considered here, both because the structure of light nuclei is much better understood than

that of the heavy nuclei, and because the electron wavefunction gradient at the nucleus is relatively small for light nuclei.

Consider the conceptually simplest variant of a PNC experiment in a hydrogenic system: circular dichroism (i.e. the difference in transition rates for right- and left-circularly polarized light) on the 1S→2S transition in the absence of external electric and magnetic fields. Dichroism arises due to interference between the $M1$ and the PNC-induced $E1$amplitudes of the transition.

Due to the PNC interaction, the 2S state acquires an admixture of the $2P_{1/2}$ state; the magnitude of the PNC admixture is probed by tuning the laser in resonance with the highly forbidden 1S→2S $M1$-transition and observing circular dichroism. Tracing Z-dependences of various atomic parameters, one finds that while the weak interaction matrix element increases $\propto Z^5$, the PNC asymmetry, i.e. the relative difference in absorption for the two circular polarizations, decreases $\propto Z^{-2}$, while the statistical sensitivity increases $\propto Z^4$ [65].

The frequencies of the 1S→2S transitions for the hydrogenic ions lie outside the range directly accessibly to laser sources. This problem can be solved by using relativistic Doppler tuning. For an ion with relativistic factor $\gamma = \frac{1}{\sqrt{1-\beta^2}} >> 1$ colliding head-on with a photon of frequency ω_{lab}, the frequency in the ion's rest frame is given by:

$$\omega_{ion\ frame} = \gamma(1+\beta)\omega_{lab} \approx 2\gamma\omega_{lab}\,. \qquad (7)$$

In order to tune to the 1S→2S resonance for a hydrogenic ion, it is necessary to satisfy the condition:

$$\Delta E_{2S-2P} \approx Z^2 \cdot 10.2 \text{ eV} = 2\gamma\hbar\omega_{lab}\,. \qquad (8)$$

Using the Relativistic Heavy Ion Collider (RHIC, $\gamma \approx 100$), with visible and near-UV lasers, it is possible to access 1S→2S transitions for ions with Z up to ≈11 (Na).

Evaluating the statistical sensitivity of the experiment, one arrives at the following expression:

$$\boldsymbol{d}H_w = \frac{1}{4}\sqrt{\frac{\Gamma_D \Gamma_{2P}}{\dot{N}_{ions} T \boldsymbol{c}_{E1}}} \quad . \tag{9}$$

Here $\Gamma_D \approx \omega_{ion\,frame} \cdot \frac{\Delta\gamma}{\gamma}$ is the Doppler width, $\dot{N}_{ions}$ is the average number of ions entering the interaction region per unit time, T is the overall measurement time, and χ_{E1} is a dimensionless saturation parameter. This shows that for an optimally designed PNC experiment, the statistical sensitivity is completely determined by the total number of available ions and by the transition widths. In order to obtain a certain sensitivity to weak interaction parameters, e.g. to $sin^2\boldsymbol{q}_w$, where $\boldsymbol{q}_w$ is the Weinberg angle, it is necessary to have exposure $\dot{N}T$ which can be represented in units of particle-Amperes×year:

$$Exposure[part.Amp \times year] \geq \frac{\Delta \boldsymbol{g}}{\boldsymbol{g}} \cdot \frac{0.1}{Z^4 \cdot (\boldsymbol{d} \sin^2 \boldsymbol{q}_w)^2 \cdot \boldsymbol{c}_{E1}} . \tag{10}$$

As an example, for $\delta \sin^2 \theta_w = 10^{-3}$, using Ne ions (Z=10) in RHIC, and substituting $\boldsymbol{c}_{E1} = 6 \cdot 10^{-2}$ (which is found to be an optimal value limited by laser photoionization), one obtains the necessary running time ~ 1 week. In this estimate we assumed $\Delta\gamma/\gamma=10^{-6}$, which is possible to achieve using laser cooling [66,65].

Many technical problems would have to be addressed before a PNC experiment could be carried out. This includes development of a hydrogenic ion source for the accelerator, implementation of laser cooling, design of an efficient detection scheme for ions excited to the 2S state, etc. However, all of these problems appear, at least in

principle, tractable, and the proposed technique may offer sensitivity sufficient for testing physics beyond the standard model.

Another promising technique involving heavy (Z up to 92) helium-like ions has been discussed in [67].

Metastable atoms in chiral boxes. In a series of recent theoretical papers [68], the authors considered hydrogen-like atoms in unstable levels of principal quantum numbers n=2 placed in segmented boxes with characteristic dimensions of several nm. Electric fields are applied in the box's segments whose direction are chosen so the whole structure is chiral (i.e. possesses a certain handedness). As could be expected in analogy with chiral molecules, there appear PNC energy shifts in such a system. What is surprising, however, is that the calculations [68] indicate that there are certain resonance values of the system's parameters corresponding to complex energy level-crossing that lead to appearance of energy shifts proportional to $\sqrt{H_W}$. This potentially gives a significant advantage compared to the usual situations where the PNC observable is $\propto H_W$. When the handedness of the system is reversed, the PNC shift is multiplied by a phase factor i, which means that the real and imaginary parts of the complex energies are interchanged. It remains to be seen whether these ideas could be realized experimentally.

Measuring nuclear-spin dependent PNC in the ground state hyperfine structure transitions of the alkali atoms. These radio frequency (rf) transitions have been discussed in the context of PNC since the 1970's [69]. In [70], experiments with polarized Cs and K atoms were considered. Recently, this proposal was reevaluated [71], leading to a concrete design of an experiment with K. There are three main advantages of such experiment in comparison with optical experiments carried out earlier. First, there is no nuclear-spin independent (NSI) PNC contribution to the amplitude and the entire PNC signal would be attributed to the nuclear-spin dependent (NSD) part of the PNC Hamiltonian. (The NSI PNC transition amplitude cancels for the case of hyperfine transitions because the NSI interaction causes equal admixtures of opposite parity states to the upper and lower level, which leads to equal and opposite contributions to the transition amplitude). Second, extremely slow electron-spin relaxation rates (~1 Hz) have been achieved for the ground state hyperfine levels of potassium [72]. This, in turn, makes it possible to achieve extremely high statistical sensitivity to the PNC signal. Third, for the isotope ^{41}K (I=3/2),

if a strong DC magnetic field is applied, the transition frequency can be as low as 60 MHz, which corresponds to a wavelength of 5 meters. Working with a 3 cm cell, it is possible to position it in the antinode of the electric field (and thus the node of the magnetic field), and thereby suppress the parity conserving magnetic dipole transition amplitude by many orders of magnitude. At high magnetic fields there is an additional suppression of the background M1 transition amplitude. By varying the DC magnetic field in the range 400 Gs - 4 kGs, one can change the amplitude of the magnetic transition by an order of magnitude, while both the transition frequency and the PNC amplitude remain essentially unchanged. This makes it possible to control the dominant spurious effects associated with the M1 amplitude (particularly, the most dangerous component having the same signature as the PNC effect under reversals). In addition, the usually troublesome spurious Stark-induced E1 transition amplitude is suppressed here by a factor of at least $<H_{hfs}>/Ry \sim 10^{-5}$ [73]. Finally, in the future it may also be advantageous to perform measurements on the other two naturally occurring isotopes of potassium with non-zero nuclear spin (^{39}K, I=3/2 and the radioactive isotope ^{40}K, I=4 with $\sim 10^9$ year half-life). Measurement of NSD constants for three nuclei, two having only an unpaired proton and one having contributions to the nuclear spin from both a proton and a neutron, can give comprehensive information on the nuclear weak interaction potential for protons and neutrons.

The basic idea of the experiment is to measure interference between the allowed $M1$ and the PNC-induced $E1$ matrix elements in the transition between the hyperfine sublevels of the ground state of K. Similar experiments with a beam of hydrogen in the 2S metastable state were discussed in the early eighties [74].

The ground state hyperfine energy levels of ^{41}K (ground state $4S_{1/2}$, nuclear spin I = 3/2) as a function of magnetic field (Breit-Rabi diagram) are shown in Fig. 16. The PNC experiment will involve a series of cycles each involving a laser light pulse for optical pumping, an electric field rf pulse (to drive the $E1_{PNC}$ amplitude), rf magnetic field pulse (to drive the reference $M1$ amplitude), a second (probe) laser pulse, and finally, detection of fluorescence light from atoms excited by the probe light pulse. Optical pumping and probing will be accomplished by circularly polarized diode laser light tuned to the D1 resonance line (λ=770 nm). Consider, e.g., left circularly polarized

light. As a result of optical pumping, all atoms will accumulate in state 2 since this is the only state decoupled from light. Since atoms are residing in a 'dark state', they will not produce fluorescence when illuminated by left circularly polarized light. When rf electric and magnetic field pulses (with rf frequency tuned to the 2→5 resonance) are applied, population of state 5 is partially replenished, so a probe laser pulse which comes after the rf pulses will produce resonance fluorescence that will be detected in the experiment. The amount of the fluorescent light is a measure of the rf transition probability.

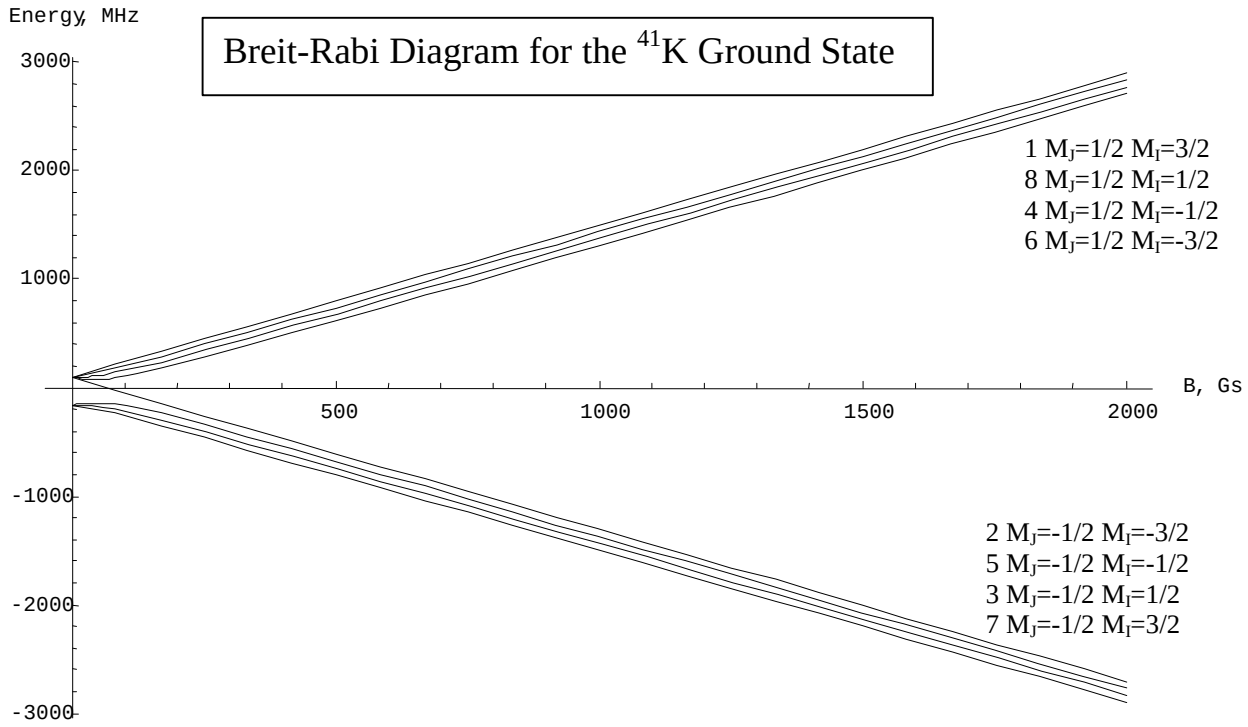

Fig. 16. Energy level diagram for the ground electronic state of potassium as a function of applied dc magnetic field. For convenience of reference, eigenstates are labeled by numbers 1 through 8. Also shown is the eigenstates' identification in the decoupled (strong-field) basis.

By either switching the polarization of light from left to right, or reversing the direction of the dc magnetic field, we can populate level 1 and look for the 1→8 transition rather than 2→5. In a high dc magnetic field the corresponding resonance frequencies are very

close. Suppose that in the rf magnetic field pulse, an oscillating magnetic field $\boldsymbol{\beta}_1 = \beta_1\cos(\omega t)\mathbf{x}$ (perpendicular to the dc magnetic field $\mathbf{B}_0$) resonantly drives the M1 transition $2\rightarrow5$ (or $1\rightarrow8$) for time τ_β, and that the field is sufficiently weak so $\mu\beta_1\tau_\beta<<1$. Next, an oscillating electric field, perpendicular to both $\mathbf{B}_0$ and $\boldsymbol{\beta}_1$ and coherent with $\boldsymbol{\beta}_1$, is applied for time τ_ε. The electric field is at the same frequency as $\boldsymbol{\beta}_1$ and has a phase offset φ: $\boldsymbol{\varepsilon}_2 = \varepsilon_2\cos(\omega t+\varphi)\mathbf{y}$. This electric field drives the PNC-induced E1 transition between the same sublevels. After these pulses, the amplitude of finding atoms in the state 5 (8) is:

$$a = a_{M1} + a_{E1} = \mu\beta_1\tau_\beta + d\varepsilon_2\tau_\varepsilon e^{i\varphi}, \tag{11}$$

where

$$\mu \cong \pm \boldsymbol{\mu}_B \cdot \frac{\sqrt{3}\Delta E_{hfs}}{4\boldsymbol{\mu}_B B_0} \tag{12}$$

is the $M1$ amplitude (the sign of this amplitude is different for transitions $2\rightarrow5$ and $1\rightarrow8$), $d \cong 2\times10^{-14}\ ea_0$ is the NSD-PNC induced $E1$ amplitude that had been calculated in [70]. Following the probe light pulse, we have a fluorescence signal proportional to the population of the level 5:

$$S \propto (\mu\beta_1\tau_\beta)^2 + 2(\mu\beta_1\tau_\beta)(d\varepsilon_2\tau_\varepsilon)\cos\varphi \quad (\text{for } d\varepsilon_2\tau_\varepsilon<<\mu\beta_1\tau_\beta). \tag{13}$$

The signal contains an interference term which is linear in the desired quantity d, which has a dominant contributions from the anapole moment and a smaller contribution from the axial-nucleon, vector-electronic Standard Model coupling. This term can be modulated by chopping the relative phase φ of the rf fields between 0 and π and observing the asymmetry:

$$A = [S(\varphi = 0) - S(\varphi = \pi)]/ [S(\varphi = 0) + S(\varphi = \pi)] = 2(d\varepsilon_2\tau_\varepsilon)/(\mu\beta_1\tau_\beta). \tag{14}$$

The interference term has the signature of the P-odd, T-even invariant $(\boldsymbol{\beta}_1\times\mathbf{B}_0)\cdot\boldsymbol{\varepsilon}_2$. In addition to chopping the relative phase between the rf fields, we thus have another available reversal: change the polarity of the magnetic field $\mathbf{B}_0$ (which has to be accompanied by a flip of circular polarization of light σ). Note also that a flip of circular polarization without reversal of $\mathbf{B_0}$ does not change the sign of the PNC asymmetry.

(With right circularly polarized light, atoms will be optically pumped to the state 1 (Fig. 11), and the rf frequency has to be slightly adjusted, so it is resonant with the $1\rightarrow 8$ transition.)

During the rf electric field pulse, there are also inevitable magnetic fields at the same (resonance) frequency. It is necessary for the experiment to keep the *M*1 transition probability due to these fields much less than the desired *M*1 transition probability $(\mu\beta_1\tau_\beta)^2<1$. If the cell of a characteristic dimension 2r is placed in the antinode of the electric field, the rf magnetic field averaged over the cell volume can be made close to zero, with maximum value at the edge of the cell being on the order of $\beta_2\sim\varepsilon_2\cdot\pi r/\lambda$. The rf magnetic field 'seen' by a particular atom in a cell without buffer gas, when averaged over the time of the pulse, will be greatly reduced due to atomic motion. This is because the atom will experience magnetic fields of different orientations in different points within the cell. This mechanism may be thought as an effective line broadening: the phase of the magnetic field 'seen' by an atom remains constant for a time $\tau_c\sim r/v$, where v is the speed of atomic thermal motion, after which it changes randomly depending on how the atom moves within the cell. The *M*1 transition probability can be estimated in this case as $(\beta_2\cdot\mu\cdot\tau_\varepsilon)^2\cdot\tau_c/\tau_\varepsilon$, i.e. atomic motion leads to additional suppression of effective rf magnetic field by a factor of $(\tau_c/\tau_\varepsilon)^{1/2}$. Using vapor cells with best anti-relaxation coatings, in which atoms survive up to several thousand wall-collisions without loss of polarization, one can thus suppress effective average magnetic field by a factor 30-100. The residual field is also reduced by choosing the transition frequency as low as possible. This favors the isotope ^{41}K with ΔE_{hfs} of only 254 MHz. Moreover, in a strong dc magnetic field ($\mu_0 B_0 >> \Delta E_{hfs}$), the transition frequency is reduced to $\sim\Delta E_{hfs}/4=64$ MHz. Working at a high dc magnetic field additionally suppresses the *M*1 amplitude due to the inverse proportionality of the amplitude (12) and the dc field B_0. For this reason, we will work at $B_0\approx 4$ kGs, which corresponds to suppression of the magnetic amplitude by two orders of magnitude. Finally, we estimate that transition probability due to the unwanted rf magnetic field β_2 which accompanies ε_2 can be kept < 1 with the following choice of the parameters: ε_2 = 1 kV/cm; 2r = 1 cm; τ_ε ~ 0.1 s. In the two rf-pulse scheme, it is necessary to apply both a rf magnetic field and a rf electric field. Taking the duration of

the rf magnetic pulse to be $\tau_\beta \approx 10^{-2}$ sec and $\mu \approx 10^{-2}\ \mu_0$ (which corresponds to $B_0 \approx 4$ kGs), the required amplitude of the rf magnetic field is $\beta_1 \approx 10^{-2}$ Gs.

Assuming a shot noise-limited measurement, the achievable statistical accuracy can be easily estimated (cf. Eq. (6) above). Assuming $\tau_\varepsilon \approx \tau$, and that the optical pumping/probing times and τ_β are much shorter than τ, and using ε_2 = 1 kV/cm, the efficiency factor f = 10%, n = 10^{11} cm^{-3}, r=.5 cm, τ=0.1 sec, one obtains that a 1% statistical determination of the NSD-PNC effect can be made in just about twenty minutes (with $\mu\beta\tau_\beta \approx 1$, these parameters correspond to an expected PNC asymmetry $A \sim 10^{-5}$). Such high statistical sensitivity comes about because of long spin relaxation time and high density that is readily achieved in a vapor cell. Clearly, the actual sensitivity of this experiment will be determined by our ability to control spurious effects. Due to availability of many reversals and possible auxiliary measurements (which can be performed very fast because of high statistical sensitivity of the experiment), we believe that it is feasible to control systematic uncertainties at a level of several percent.

Implications of atomic PNC experiments in particle physics, conclusion and optimistic outlook

The results of atomic PNC experiments, particularly those of the Boulder Cs experiment, play an important role in probing physics beyond the standard model when they are combined with the high-precision high-energy data. This is illustrated in Table 1.

New Physics	Parameter	Constraint from atomic PNC	Direct constraints from HEP	References
Oblique radiative corrections	S+0.006T	-1.0±1.2	S = -0.28±0.19, T = -0.20±0.26	75, 76, 77, 78
Z_x-boson in SO(10) model	M (Z_x)	>550 GeV	>425 GeV	79, 76, 78
Leptoquarks	M_S	>0.7 TeV	>0.28 TeV	77
Composite Fermions	$\boldsymbol{L}$	>14 TeV	>6 TeV	77

Table 1. Limits on new physics beyond the standard model currently obtained from atomic PNC and directly from high-energy physics (HEP).

There are all reasons to believe that atomic PNC will continue to be an effective tool for probing limits of the standard model, complementing efforts at high-energy facilities. An even more spectacular impact of atomic PNC is likely to be in nuclear physics, where

anapole moments of a variety of nuclei will probably be measured in the next several years. Now a quarter of a century old, experimental atomic PNC remains a vibrant, productive, cutting edge area of multidisciplinary research.

Acknowledgements

I am indebted to C. J. Bowers, E. D. Commins, D. DeMille, V. V. Flambaum, E. N. Fortson, D. F. Kimball, M. G. Kozlov, A.-T. Nguyen, J. E. Stalnaker, P. A. Vetter, R. B. Warrington, C. E. Wieman, and M. Zolotorev for their help in preparation of this review. This work has been supported by UC Berkeley Committee on Research and by the Nuclear Science Division, LBNL.

♣ E-mail: budker@socrates.berkeley.edu

[1] Ya. B. Zel'dovich, Sov. Phys. JETP **9**, 682 (1959).
[2] Znakomyi neznakomyi Zeldovich: v vospominaniiakh druzei, kolleg, uchenikov (in Russian), Moskva: Nauka, 350 pp.
[3] M.-A. Bouchiat and C. Bouchiat, Phys. Lett. **48B**, 111 (1974); J. Phys. (Paris) **35**, 899 (1974); J. Phys. (Paris) **36**, 483 (1975).
[4] L. M. Barkov and M. Zolotorev, JETP Lett. **27**, 357 (1978); JETP Lett. **28**, 503 (1978); Phys. Lett. **B 85**, 308 (1979).
[5] R. Conti, P. Bucksbaum, S. Chu, E. Commins, and L. Hunter, Phys. Rev. Lett. **42**, 343 (1979).
[6] D. B. Cline, Ed. Weak Neutral Currents. The Discovery of the Electro-weak Force. Addison-Wesley, 1997.
[7] P. Langacker, in: Precision tests of the Standard electroweak model, P. Langacker, ed., World Scientific, 1995.
[8] Ya. B. Zel'dovich, Sov. Phys. JETP **6**, 1184 (1958).
[9] V. V. Flambaum and I. B. Khriplovich, Sov. Phys. JETP **52**, 835 (1980); V. V. Flambaum, I. B. Khriplovich, and O. P. Sushkov, Phys. Lett. B **146**, 367 (1984).
[10] C. S. Wood, S. C. Bennett, D. Cho, B. P. Masterson, J. L. Roberts, C. E. Tanner, and C. E. Wieman, Science **275**, 1759 (1997).
[11] E. G. Adelberger and W. C. Haxton, Annu. Rev. Nucl. Part. Sci. **35**, 501 (1985).
[12] S. J. Pollock, E. N. Fortson, and L. Wilets, Phys. Rev. C **46**, 2587 (1992); E.N. Fortson, Y. Pang, and L. Wilets, Phys. Rev. Lett. **65**, 2857 (1990).
[13] I. B. Khriplovich, Parity Non Conservation in Atomic Phenomena (Gordon and Breach, Philadelphia, 1991).
[14] D. N. Stacey, in *Atomic Physics 13*, eds. H. Walther, T. W. Hansch and B. Neizert (New York: AIP) 46 (1993); E. D. Commins, Physica Scripta **T46**, 92 (1993); P. E. G. Baird, in Physics with Multiply Charged Ions, ed. D. Liesen, NATO ASI Series, Series B:Physics Vol. 348 (Plenum, New York, 1995), p. 87; M. A. Bouchiat, in Atomic Physics 12, eds. J. C. Zorn and R. R. Lewis (AIP, New York, 1991), p. 399.
[15] M.-A. Bouchiat and C. Bouchiat, Rep. Prog. Phys. **60** (11), 1351 (1997).
[16] M. G. Kozlov and L. N. Labzovsky, J. Phys. B. **28**(10), 1933 (1995).

[17] M. J. D. McPherson, K. P. Zetie, R. B. Warrington, D. N. Stacey, and J. P. Hoare, Phys. Rev. Lett. **67**(20), 2784 (1991).
[18] P. Vetter, D. M. Meekhov, P. K. Majumder, S. K. Lamoreaux, and E. N. Fortson, Phys. Rev. Lett. **74**, 2658 (1995).
[19] D. M. Meekhof, P. A. Vetter, P. K. Majumder, S. K. Lamoreaux, and E. N. Fortson, Phys. Rev. A **52**(3), 1895 (1995).
[20] Since in the wing of a line, absorption goes as$1/\Delta^2$, where Δ is the frequency detuning, and optical rotation goes as $1/\Delta$, a net rotation enhancement can be achieved in the wing at the expense of loosing information in the line center due to complete absorption.
[21] V. A. Dzuba, V. V. Flambaum, P. G. Silvestrov, and O. P. Sushkov, J. Phys. B: *At. Mol. Phys.* **20**, 3297 (1987).
[22] V. A. Dzuba, V. V. Flambaum, and M. G. Kozlov, Phys. Rev. A **54**(5), 3948(1996); JETP Lett., **63**(11), 882(1996).
[23] V. A. Dzuba, V. V. Flambaum and I. B. Khriplovich, Z. Phys. **D1**, 243 (1986).
[24] B. Q. Chen and P. Vogel, Phys. Rev. C **48**(3), 1392 (1993); S. J. Pollock, in Future Directions in Parity Violation, Fifth Annual JLAB (CEBAF)/INT Workshop, June 22-24, 1997, R. Carlini and M. J. Ramsey-Musolf, eds. Washington, INT 1997.
[25] V. A. Dzuba, V. V. Flambaum, and O. P. Sushkov, Phys. Lett. **141A**, 147 (1989); S. A. Blundell, W. R. Johnson, and J. Saperstein, Phys. Rev. Lett. **65**, 1411 (1990); Phys. Rev. D **45**, 1602 (1992).
[26] V. V. Flambaum and D. W. Murray, Phys. Rev. C. **56**(3), 1641 (1997); Austr. New Zeal. Physicist **34**(5/6), 82 (1997).
[27] Note that in this case, in contrast to a single loop, the magnetic field produced by the current is confined within the torus, so a "contact" interaction is needed to probe it. In addition, the value of the anapole moment does not depend on the choice of the origin. The situation here is analogous to a single charge offset from the origin and a dipole formed by two opposite charges. One may say that the toroidal current is the simplest example of an "irreducible" anapole.
[28] S. L. Gilbert and C. E. Wieman, Phys. Rev. A, **34**(2), 792 (1986).
[29] M. A. Bouchiat, P. Jacquier, M. Lintz, and L. Pottier, Opt. Commun. **56**, 100 (1985); Ibid. **77**, 374 (1990); J. Guena, D. Chauvat, P. Jackier, M. Lintz, M. D. Plimmer, and M. A. Bouchiat, J. Opt. Soc. Am. B. **14**, 271 (1997).
[30] D. DeMille, Phys. Rev. Lett. 74, 4165 (1995).
[31] S. Porsev, Yu. Rakhlina, and M. Kozlov, JETP Lett. **61**, 459 (1995); B. P. Das, Phys. Rev. A **56**(2), 1635 (1997).
[32] A. D. Singh and B. P. Das, private communication (submitted for publication).
[33] I. B. Khriplovich, private communication (1995).
[34] C.J. Bowers, D. Budker, D. DeMille, et. al., Phys. Rev. A 53 (5), 3103(1996).
[35] C. J. Bowers, Ph. D. Thesis, Berkeley, 1998; C. J. Bowers et al, in preparation; J. E. Stalnaker, Undergraduate Thesis, Berkeley, 1998.
[36] N. A. Kryukov, N. P. Penkin, and T. P. Redko, Opt. Spectrosc. **66**(6), 719, 1989; N. A. Kryukov, P. A. Savel'ev, and M. A. Chaplygin, Opt. Spectrosc. **82**(5), 747, 1997.
[37] D.DeMille, D.Budker, E.Commins, and M.Zolotorev, in: Particle Astrophysics, Atomic Physics and Gravitation, ed. by J. Tran Thanh Van, G. Fontaine, and E. Hinds, Editions Frontieres, 1994.

[38] W.C. Martin, R. Zalubas and L. Hagan, Atomic Energy Levels-The Rare Earth Elements (National Bureau of Standards, Washington, DC., 1978).
[39] D. Budker, D.DeMille, E.D. Commins and M.S. Zolotorev, Phys. Rev. Lett. 70, 3019 (1993); Phys. Rev. A 50(1), 132, (1994).
[40] R.R. Lewis and W.L.Williams, Phys. Lett. B59, 70 (1975).
[41] A.-T. Nguyen, D. Budker, D. DeMille, and M. Zolotorev, Phys. Rev. A **56**(5), 3453 (1997).
[42] V.A. Dzuba, V.V. Flambaum, and M.G. Kozlov, Phys. Rev. A **50**, 3812 (1994).
[43] D. Budker, D.DeMille, E.D. Commins and M.S. Zolotorev, Phys. Rev. Lett. **70**, 3019 (1993); Phys. Rev. A **50**(1), 132, (1994).
[44] V. V. Flambaum and M. G. Kozlov, private communications.
[45] D.E. Brown and D. Budker, in preparation.
[46] A. Gongora and P. G. H. Sandars, J. Phys. B **19**, 291 (1986).
[47] L. M. Barkov, M. S. Zolotorev and D. A. Melik-Pashaev, Opt. Spektrosk. **66**, 495 (1989) [Opt. Spectrosc. (USSR) **66**, 288 (1989)].
[48] I. O. G. Davies, P. E. G. Baird, P. G. H. Sandars and T. D. Wolfenden, J. Phys. B. **22**, 741 (1989).
[49] T. D. Wolfenden and P. E. G. Baird, J. Phys. B **26**, 1379 (1993); Addenda: J. Phys. B **26**, 2229(1993).
[50] D. M. Lucas, D. N. Stacey, C. D. Thompson and R. B. Warrington, Phys. Scripta **T70**, 145 (1997); D. M. Lucas, R. B. Warrington, D. N. Stacey and C. D. Thompson, submitted to Phys. Rev. A.
[51] D. Burrow and R.-H. Rinkleff, The Arabian Journal for Science and Engineering **17**, 287 (1992).
[52] T. Kobayashi, I. Endo, et. al., Z. Phys. D **39**, 209 (1997).
[53] A. Fukumi, I. Endo, et. al., Z. Phys. D **42**, 237 (1997).
[54] S. M. Rochester, Undergraduate Thesis, Berkeley, 1998; S. Rochester et al, in preparation.
[55] L. N. Labzovskii and O. A. Mitruschenkov, Sov. Phys. JETP **67**, 1749 (1988); M. G. Kozlov and S. G. Porsev, Sov. Phys. JETP **70**(1), 85 (1990).
[56] A. D. Cronin, R. B. Warrington, S. K. Lamoreaux, and E. N. Fortson, Phys. Rev. Lett. **80**(17), 3719 (1998).
[57] K.-J. Boller, A. Imamoglu, and S. E. Harris, Phys. Rev. Lett. **66**, 2593 (1991); S. E. Harris, Phys. Today **50**(7), 36 (1997).
[58] In principle, if many Watts of the 535 nm light power were available, a bleaching technique could be used to reduce this problem (E. N. Fortson, private communication).
[59] E. N. Fortson, Phys. Rev. Lett. **70**, 2383 (1993).
[60] E. N. Fortson, private communication (1998).
[61] E. V. Stambulchik and O. P. Sushkov, Phys. Lett. A **158**, 295 (1991); V. V. Flambaum and O. P. Sushkov, Phys. Rev. A **47**(2), R751 (1993).
[62] C. E. Wieman, Hyperfine Int. **81**, 27 (1993).
[63] G. D. Sprouse, L. A. Orozco, J. E. Simsarian, W. Z. Zhao, Nucl. Phys. A **630**(1-2), 316 (1998); Z.-T. Lu, K. L. Corwin, K. R. Vogel, C. E. Wieman, T. P. Dinneen, J. Maddi, and H. Gould, Phys. Rev. Lett. **79**(6), 994 (1997).
[64] E. Hinds, in *The Spectrum of Atomic Hydrogen: Advances*, ed. G. W. Series (World Scientific, Singapore, 1988).

[65] M. Zolotorev and D. Budker, Phys. Rev. Lett. **78**(25), 4717 (1997).
[66] D. Habs, V. Balykin, M. Grieser, R. Grimm, E. Jaeschke, M. Music, W. Petrich, D. Schwalm, A. Wolf, G. Huber, and R. Neumann, in *Electron Cooling and New Cooling Techniques*, R. Calabrese and L. Tecchio, eds, World Scientific, Singapore, 1991.
[67] R. W. Dunford, Phys. Rev. A **54**(5), 3820 (1996).
[68] D. Bruss, T. Gasenzer, and O. Nachtmann, Phys. Lett. A, **239**(1-2), 81 (1998); E-print archive hep-ph/9802317 (1998).
[69] V. N. Novikov and I. B. Khriplovich, JETP Lett. **22**, 74 (1975); V. E. Balakin and S. I. Kozhemyachenko, JETP Lett. **31**, 326 (1980); A. Ya. Kraftmakher, Preprint 90-54, Institute of Nuclear Physics, Novosibirsk (1990).
[70] V. G. Gorshkov, V. F. Ezhov, M. G. Kozlov and A.I.Mikhailov, Sov. J. Nucl. Phys.,**48**(5), 867 (1988)
[71] D. DeMille, unpublished; E. B. Alexandrov, M. V. Balabas, D. Budker, D. DeMille, M. G. Kozlov, V. V. Yashchuk, V. F. Yezhov, M. Zolotorev, et al, in preparation.
[72] E. B. Alexandrov, M. V. Balabas, A. S. Pasgalayev, A. K. Verkhovskii, and N. N. Yakobson, Laser Physics **6** (2), 244 (1996).
[73] M. G. Kozlov and D. DeMille, submitted for publication (1998).
[74] E.G.Adelberger *et* al, NIM, **179**,181, (1981); R.T.Robiscoe and W.L.Williams, NIM, **197**, 567 (1982).
[75] M. E. Peskin and T. Takeuchi, Phys. Rev. D **46**, 381 (1992).
[76] V. A. Dzuba, V. V. Flambaum, and O. P. Sushkov, Phys. Rev. A **56**(6), R4357 (1997).
[77] M. J. Ramsey-Musolf, in Future Directions in Parity Violation, Fifth Annual JLAB (CEBAF)/INT Workshop, June 22-24, 1997, R. Carlini and M. J. Ramsey-Musolf, eds. Washington, INT 1997.
[78] Review of Particle Physics. Particle Data Group, 1996.
[79] W. J. Marciano and J. L. Rosner, Phys. Rev. Lett. **65**, 2963 (1990).